Copy 6
RM E53E21

NACA RM E53E21

NACA

RESEARCH MEMORANDUM

MECHANICAL DESIGN ANALYSIS OF SEVERAL NONCRITICAL AIR-COOLED TURBINE DISKS AND A CORRUGATED-INSERT AIR-COOLED TURBINE ROTOR BLADE

By Merland L. Moseson, Morton H. Krasner
and Robert R. Ziemer

Lewis Flight Propulsion Laboratory
Cleveland, Ohio

NATIONAL ADVISORY COMMITTEE
FOR AERONAUTICS

WASHINGTON

July 22, 1953

NACA RM E53E21

NATIONAL ADVISORY COMMITTEE FOR AERONAUTICS

RESEARCH MEMORANDUM

MECHANICAL DESIGN ANALYSIS OF SEVERAL NONCRITICAL AIR-COOLED TURBINE DISKS AND A CORRUGATED-INSERT AIR-COOLED TURBINE ROTOR BLADE

By Merland L. Moseson, Morton H. Krasner, and
Robert R. Ziemer

SUMMARY

As a part of the NACA investigations of air-cooled turbines, a series of turbine wheel designs was made for a turbojet engine with an axial-flow compressor. These designs were made to determine the influence of air-cooling on over-all engine design, weight, critical-material content, and complexity as well as to provide necessary information for the construction of research model full-scale turbines. The effect of air-cooling on these factors is illustrated by the five designs presented in this report, which include the principal variations in methods of cooling-air introduction and distribution. The mechanical design, construction, and stresses of the corrugated-insert air-cooled blade utilized in all the disk designs are included. The disk designs considered are both the split-type disk and the single disk with a cooling-air shroud. All parts were designed for use of noncritical materials for applications using current turbine-inlet temperature levels. Component and total turbine wheel weights are also presented. Reductions of critical-material content as compared with uncooled designs were shown to be approximately 93 percent.

INTRODUCTION

Investigations for air-cooling gas-turbine blades have been conducted at the NACA Lewis laboratory for the purpose of reducing the critical-material content, increasing the gas-temperature level, or permitting higher operating stresses in the blades. Configurations of alternate types of air-cooled turbine rotor blades having been reasonably well defined, the next phase of the research was directed toward answering the following question: To what extent will it be necessary to alter existing engine design concepts in order to incorporate air-cooling in flight model engines? A specific and related problem is the effect of

air-cooling on engine arrangement, strength, weight, critical-material content, and producibility. As a preliminary step in this phase of the investigations, a design study was made based on using noncritical materials in the rotor blades and disks for application with current turbine-inlet gas-temperature levels. An air-cooled blade configuration having good cooling characteristics was selected for this study, and all the turbines compared were identical with respect to shape, size, and number of air-cooled turbine rotor blades.

Prior investigations (refs. 1 and 2) have been conducted on air-cooled blades similar to the blade used herein. These investigations indicate that the corrugated-insert blade as well as the 10-tube blade of reference 3 and the strut blade of reference 4 would be suitable for one or more of the general purposes for utilizing cooled blades.

In addition to obtaining air-cooled blades that have high cooling effectiveness and acceptable stress levels, the problem of supplying the cooling air to the blades has also been considered. Previous experimental research on air-cooled turbine rotors (refs. 5 and 6) utilized a split-disk construction, the cooling-air being introduced through the downstream face of the turbine disk. For this application, several other types of construction that were considered are presented schematically in reference 7. These alternate designs, however, were not evaluated in the light of disk stress analysis and the resulting weight comparison.

All the turbine designs considered herein utilize the corrugated-insert air-cooled blade of reference 2 (configuration H; profile 2). The profile of this blade was evolved in an effort to obtain good cooling effectiveness and to simplify fabrication procedures. In so doing, the specified profile was quite thick in the midchord region and the trailing-edge section. A complete description of this blade design and the results of a performance investigation in cold air of a small-scale model of the turbine are presented in reference 8. The cooling characteristics of this corrugated-insert blade are presented in the heat-transfer and cooling-air flow analysis of reference 2.

The assumption is made for the design studies presented herein that provision for turbine cooling would be incorporated into the original layout of the engine. The mechanical design, stress analysis, and method of fabrication of the corrugated-insert blade are discussed in the present report, with consideration given to both tapered and untapered blade shells and three types of root fastening. Five disk designs for use with this blade are included to illustrate variations in methods of distribution and introduction of cooling air to the blades. Representative types of configuration for introducing the cooling air into the turbine disks are also shown. These designs indicate generally the requirements for incorporating turbine rotor and rotor blade cooling in an engine design. For comparative value, all work was based on the same turbine tip diameter

of 33.5 inches and speed of 8000 rpm. The results obtained, however, can be generalized to a large extent and should be useful to anyone designing a turbojet engine that will incorporate an air-cooled turbine rotor. In the designs presented herein, it is acknowledged that prior library reviews of the many German designs, such as those presented in reference 9, may have left their influence.

SYMBOLS

The following symbols are used in this report:

A cross-sectional metal area, sq in. or sq ft

a constant

b constant

D diameter of bearing bore, mm

g acceleration due to gravity, ft/sec^2

N speed, rpm

n exponent in temperature-gradient equation, dimensionless

r radius, in.

T temperature, ^oF

V velocity, ft/sec

β angle between radial line and line of bearing contact (see fig. 5)

ρ metal density, lb/cu in.

σ stress, psi

Subscripts:

e equivalent

r radius or radial

T blade tip

t tangential

DESIGN OF AIR-COOLED TURBINE ROTOR BLADE

The design requirements of a good noncritical, air-cooled blade include high cooling effectiveness, good aerodynamic performance, acceptable stresses, fabrication simplicity, and light weight. The airfoil considered here and shown in figure 1 fulfills these requirements to a greater degree than the earlier type of airfoil reported in reference 3. Since the aerodynamic design requirements of this rotor blade were the same as those of the turbine of a contemporary turbojet engine (ref. 8), the rotor blade solidity was maintained constant. The need of a thick trailing edge to ease the cooling-air distribution problem dictated the use of fewer blades in order to obtain the required work and to pass the compressor mass flow. The airfoil design was made on the basis of 72 blades having a constant-cross-section cooling-air passage; and since the solidity was maintained constant, the axial chord was increased from 1.92 to 2.25 inches. The effect of the diminished aspect ratio on turbine performance is not known, but believed to be small. The thick trailing edge of this blade and the fact that the airfoil section was untwisted tend to ease the fabrication problems. The results of an aerodynamic investigation of this blade profile in a small-scale cold-air turbine, which are presented in reference 8, show efficiencies of 82 percent at the design point. The coolant-passage configuration of the airfoil in figure 1 was the result of the analysis presented in reference 2. Reference 2 indicates that good cooling effectiveness and low pressure drop could be obtained with this blade by the use of an insert to block the central part of the coolant passage and corrugations between the insert and shell to provide additional heat-transfer area. Both analytical (ref. 2) and experimental (ref. 1) investigations indicate that the cooling-air requirements for the corrugated-insert blade are approximately 2 percent of the compressor mass flow. This cooling-air requirement is lower than that of the 10-tube blade of reference 3. Early consideration was therefore given to fabrication methods required for quantity production of this blade.

Airfoil Section

Construction. - The airfoil section of the corrugated-insert blade (fig. 1) is constructed entirely of a light-gage sheet metal. The outer shell (aerodynamic profile) is formed from tubing. The corrugations, which act as fins to increase the heat-transfer surface area, are brazed to the outer shell and the insert. These corrugations were laid out for construction by gear rolls, and, when the results of model fabrication are considered, this system of manufacturing is feasible for the corrugation configuration used. The insert reduces the cooling-air flow area and directs all the cooling air closer to the outer shell where it is most effective.

In both the untapered and tapered airfoil shells, the corrugations and insert were of uniform thickness. This uniformity provided for simple fabrication; and the analysis of reference 2 indicated that, for the stress and temperature levels imposed and for a nominal cooling-air flow ratio, the blade would be structurally adequate.

In model fabrication, Nicrobraz has been used throughout for brazing the shell, corrugations, insert, and connecting the airfoil to the base. Copper braze is a possible alternate to Nicrobraz for attaching the corrugations and insert inside the airfoil, as the shear stresses are very low in these locations. Where metal temperatures may exceed the approximately 1050° F limit imposed by the use of noncritical materials, copper braze may be ruled out according to the required shear strengths.

The use of sheet-metal construction for air-cooled turbine blades makes additional sources of manufacturing techniques and equipment available. In addition, relatively light-duty equipment will suffice for manufacturing sheet-metal blade components as compared with equipment normally used for current production of turbine blades.

Airfoil stresses. - Two variations of the blade shell were considered, one with a uniform shell thickness of 0.018 inch from root to tip and another with a shell tapering from a thickness of 0.042 inch at the root to 0.018 inch at the tip. The span and axial chord of the blade, as well as the operating temperature and speed of the turbine, are given in table I. In the stress calculations for both the tapered and untapered shells, it was assumed that all the metal in the blade cross section, shell, corrugations, and insert was integrally brazed and carried its own proportionate share of the load. The airfoil section is brazed into a 0.20-inch-deep recess in the blade base (see figs. 1 and 5), and the load from the corrugations and insert is transferred to the shell in this region and from the shell, by shear through the braze material, to the blade base.

The stresses in the airfoil section of turbine blades were calculated from the following equation, which was derived for the case in which the blade cross-sectional area distribution varied linearly along the blade span:

$$\sigma = \frac{12\rho V_T^2}{g}\left\{\frac{1}{2}\left[1 - \left(\frac{r}{r_T}\right)^2\right] - \frac{1}{3}\frac{\left[1 - \left(\frac{r}{r_T}\right)^3\right]}{1 - \frac{r}{r_T}}\left(1 - \frac{A_T}{A}\right) + \frac{1}{2}\left[\frac{r}{r_T} + \left(\frac{r}{r_T}\right)^2\right]\left(1 - \frac{A_T}{A}\right)\right\} \quad (1)$$

A graphical representation of equation (1) is given in figure 2. From figure 2 and the data in table I, the spanwise variations of centrifugal stress in both the untapered- and tapered-shell blades are plotted in figures 3(a) and (b), respectively. The tensile stress at the top of the fillet in the root region of the blade with the tapered shell is 20,600 pounds per square inch, or 19.2 percent lower than that of the constant-cross-section blade, which has corresponding stress of 25,500 pounds per square inch. A more significant effect of tapering the outer shell results when an assumed failure of the braze between corrugations and outer shell occurs in the region of that portion of the shell which extends into the base. Under these circumstances, all the airfoil load has to be carried by the outer shell, and the tensile stresses in the shell root become 61,800 pounds per square inch for the untapered shell and 33,350 pounds per square inch for the tapered shell. This comparison of stresses shows that a high-quality uniform braze is required between the components of the blade, particularly at the root section, before the use of untapered stock can be considered for turbine blades.

A summary of the blade-shell stresses is included in table II. For the blade material considered, Timken 17-22A(S), the specified heat treatment gives a hardness of Rockwell C-34. For any average blade temperature less than 1070° F, figures 3 and 4 indicate that in the region just above the base fillet there is a safety factor of 2.0 or greater, based on the 100-hour data, when the specified heat treatment is used. The stress-to-rupture properties of sheet stock will be somewhat lower than those for hot-rolled bar stock, which are presented in figure 4. The bar-stock data, however, are all that are currently available.

Base Section

The three bases shown in figure 5 were designed to provide a suitable air passage between the disks and the blade airfoil with a minimum of weight.

Two-serration cast base. - The base shown in figure 5(a) with the blade in figure 2 has two load-carrying serrations that are identical in contour and spacing to the top two serrations (nearest the root section of the blade) on the production model J33 blade bases. The inherent light-weight construction of the corrugated-insert air-cooled blade and a minimized depth of radial slots required in the disks for the bases tend to reduce dead weight and make lighter disk design possible. The purpose of the bulkhead, which is shown passing through the cooling-air passage in the base, is to resist collapsing loads due to the tangential component of centrifugal force on the blade and, in some instances, compressive rim stresses in the disk due to radial thermal gradients existing in the disk material during engine operation. The integrally cast fillet on the base platform provides for increased braze area between

the blade shell and the base and also effects a gradual change in cross section from the base platform to the blade shell. This cast fillet is blended with the airfoil surface after assembly with a copper-silver braze.

According to table II and figure 5(a), the approximate tensile stress at sections M-M and N-N are 9040 and 6890 pounds per square inch, respectively, when used with the tapered shell. The bearing stress on the projected areas of the serrations (dimension P in fig. 5(a)) is 21,500 pounds per square inch. The collapsing load component of the centrifugal force is 2040 pounds, and the average shear stress in the serrations is 15,800 pounds per square inch. Comparison of these stresses with the short-time yield and stress-rupture properties on figure 4 indicates that reasonable margins of safety are provided. For example, at a blade base temperature of 1000° F, the 100-hour stress-to-rupture value for this material is 74,000 pounds per square inch; and when 50 percent of this value is assumed to be shear strength, the factor of safety is 2.34.

Single-lug cast base. - An alternate base design shown in figure 5(b) is arranged for the same depth of radial cut in the disk as for the two-serration base. The principal advantages of this single-lug base as compared with the two-serration design are the lower cost of producing broaches and crush grinding rolls and the better adaptability to the use of brittle materials. This base utilizes the same integrally cast fillet and bulkhead as the two-serration cast base. According to table II and figure 5(b) for use with the tapered shell, the tensile stress across the neck of the root section M-M is 11,280 pounds per square inch, which is only slightly greater than that for the two-serration base. The bearing stress on the projected area, dimension P, is 32,300 pounds per square inch, which is somewhat larger than that for the two-serration base, but not excessive; and the average shear stress is 12,400 pounds per square inch. The primary disadvantage found in the analysis of this single-lug base was the greater crushing load on the base due to the decreased angle β (see fig. 5) between the line of bearing contact on the lug and a radial line. The tapered-blade centrifugal load, resolved into its tangential component, gives a crushing force of 12,400 pounds, which is approximately six times as great as that for the two-serration base. Although the same shape of bulkhead is used, its need is much more critical than for the two-serration base. This base weighs 0.213 pound as compared with 0.208 pound for the two-serration base.

Six-serration cast base. - The base shown in figure 5(c) is for use with narrow-rim disks designed for plate construction. In this case the same six-serration root form as on the production model J33 turbine is used; however, as shown in figure 5(c), in the center region all but the top of these serrations are cut away. The centrifugal blade loading is carried by a larger number of active serrations than the previous serrated base discussed, in order to distribute the load into a narrow-rim disk

with similar stress levels in the root fastening. In a disk design presented later, there is no rim section in the disks for the midchord regions of the blade. The weight of this base design is 0.261 pound or 25.5 percent heavier than the two-serration base. A slight reduction in this base weight could have been accomplished by omitting the bottom serration, since the stress levels indicated in table II are somewhat lower for this base.

Choice among any of the three base designs presented is dependent upon the type of disk construction and material characteristics, rather than on any of the relative advantages inherent in a particular blade base design.

DESIGNS FOR AIR-COOLED TURBINE DISKS

An essential phase of the research on air-cooled turbines is the investigation of problems associated with introduction and distribution of cooling air to rotor blades. The designs presented in this report were made to determine the influence of air-cooling on over-all engine design, weight, critical-material content, and complexity, as well as to provide necessary information for the construction of research-model full-scale turbines. All designs presented are specifically for use with the corrugated-insert air-cooled blade shown in figure 1.

The following factors were primary considerations in all the designs:

(1) Method of providing for cooling-air inlet passages and seal at the disk entrance

(2) Uniform air distribution to each blade and throughout each blade

(3) Structural strength

(4) Critical-material content

(5) Effect on weight

(6) Effect on producibility

(7) Effectiveness of cooling-air entrance vanes

In this study, blade-fastening methods were employed that permit replacing blades, and no consideration was given to providing the lightest weight design that might be obtained by using an integral blade and disk structure.

The engine operating data of table I and the radial temperature gradient plotted in figure 6 were used to provide a basis for comparison of the disks. The stresses in the turbine disks were calculated by the methods presented in references 10 and 11. The temperature gradient was established by assuming a temperature of 400° F at a radius of 1.0 inch as a concession to easing the turbine-bearing temperature problem. A rim temperature of 1000° F was assumed, since reference 6 indicates that the rim temperatures of air-cooled turbine disks will probably be 1000° F or lower for present-day turbine-inlet temperatures and since this temperature represents the maximum temperature at which the noncritical disk material Timken 17-22A(S) has a useful strength. The radial temperature gradient used in the turbine disk stress calculations can be represented by the equation

$$T = a + br^n \tag{2}$$

where the values of the constants a and b are determined by simultaneous solution when corresponding values for T and r are substituted at the disk hub and the disk rim. For these calculations, the exponent n was assumed to be 3, which is consistent with the temperature gradient measured in the experimental investigation of the split-type disk reported in reference 6. Also shown in figure 6 are the yield strength and stress-rupture data for a noncritical material (Timken 17-22A(S)) plotted against disk radius for the assumed temperature gradient. These curves indicate that for all radii below 11.2 inches, short-time yield-strength data are the proper criteria for disk designs of this particular radial temperature gradient and material. The values for rim loading (or total centrifugal force due to all metal in the blades and interrupted portions of the disk rim divided by the peripheral area at the maximum diameter of the continuous portion of the disk) range from 12,700 pounds per square inch to 18,600 pounds per square inch for the disk stress plots that are included. These values were computed for the untapered-shell blades in each case; however, the effect of using tapered-shell blades was calculated to be an additional 1000 pounds per square inch, which is not significant in this range of rim loading. In this case, the tapered-shell design is heavier than the untapered-shell design, because 0.018 inch was the assumed minimum metal thickness that could be tolerated anywhere in the airfoil, and, since this was the thickness used for the uniform shell, the tapered-shell thickness had to be increased at the root section.

Two general types of disk are considered: the split disk, in which two similar disks share the blade loading and provide the cooling passage between them, and the single disk, which employs some variation of a lightweight shroud attached to one face to introduce and to distribute the cooling air to the blades.

Split-Type Disk

A chief advantage of the split-type air-cooled disk is that the coolant flow passages through the disk lie directly under the axial center of the blade bases and thus facilitate more uniform distribution of cooling air to the leading- and trailing-edge regions of the blades. With the split-type disk, it is generally easier to control the cooling-air flow passage areas and to provide for uniform distribution to each blade by means of either an integral or a removable set of vanes between the disks with individual passages to each blade.

In the split-type disk, pressure losses in the cooling-air flow passages will normally be less because of fewer or more gradual turns than in the case of the single disk with an exterior shroud. The optimum effectiveness required of the cooling-air vane system as a compressor has not been determined quantitatively in terms of the mechanical complexity that may be required to achieve it. The need of impeller vanes that provide an acceptable angle of attack for the cooling air and, to some extent, simulate a centrifugal compressor, is somewhat dependent on the available supply pressure and the amount of cooling air required. For example, the cooling-air flow path described in reference 6, which provided a good angle of attack for the cooling air, indicates that the pressure losses within the rotor could be ignored at coolant-flow ratios of 3 percent or below. Unpublished results on cooling-air vanes having a similar flow path but with straight radial passages (unfavorable angle of attack) show similar losses at the low coolant-flow ratios. At higher coolant-flow ratios (about 10 percent), however, the pressure losses in the straight passages were much greater than those shown in reference 6. Coolant-flow ratios of this magnitude might be required for certain missions of high-performance aircraft with engines using the corrugated-insert air-cooled turbine rotor blade.

The split disk of the type considered herein is inherently weak in resisting the gyroscopic couples set up during high-speed maneuvers, since only one of the disks can be integrally attached to the shaft and it must therefore carry its mate to a large extent. The axial temperature gradient between the forward and rear disks can pose another serious problem, as shown in reference 5. In this case, the rear disk, which had a higher temperature level, expanded more than the forward disk, and the entire load of the blades was shifted to the forward disk as well as part of the load of the rear disk.

Split disk with rear cooling-air entrance. - The air-cooled disk shown in figure 7 (the only design presented herein that has been fabricated) is arranged so that the cooling air is introduced through a 4-inch-diameter central hole in the rear disk. This size hole gives reasonable flow velocities for any condition likely to be encountered in service with this blade design. A cooling-air passage for each blade is integrally machined in the disks to ensure equitable distribution of the

cooling air to the blades and good entrance flow conditions into the blade bases and to provide some measure of pumping action. The general design of this disk is similar to that described in references 5, 6, and 7. No concerted effort was made to minimize weight in this design, because the disks in figure 7 were constructed as a research vehicle for blade- and disk-cooling heat-transfer studies and not for research on minimum-weight disk designs. Examination of figure 7 will show that the 72 cooling-air passages nearest the rim are constant-width radial elements, while the 36 curved vanes near the hub provide an acceptable angle of attack. The small interruption between the two sets of vanes is primarily to equalize flow in all passages, and it permits tool run-out during the machining of the curved inducer vanes. The single-lug blade-root attachment (fig. 5(b)) is used on this disk.

The results of elastic-stress calculations for the rear half of the disk are presented in figure 8. Centrifugal stresses in the forward disk (not included) are lower in the central regions because of the smaller central hole. In these calculations, the vanes were treated as dead load, and their contribution to the radial strength of the disk was neglected. Both the tangential and radial stresses appear reasonable when compared with the calculations presented in figure 10 of reference 7. In reference 7, the reliability of the calculation methods used for split-type disks was verified by the results of a spin-test rotor in which the calculated and actual burst speeds compared favorably.

The equivalent stress, which was calculated for the turbine disks considered, is defined in reference 11 as

$$\sigma_e = \sqrt{\sigma_r^2 - \sigma_r\sigma_t + \sigma_t^2} \qquad (3)$$

By means of the equivalent stress defined by equation (3), the calculated biaxial stresses in a disk can be compared with material properties obtained from uniaxially loaded test specimens. It is noted that, even for the rear disk of figure 7 having the central hole, the equivalent stresses throughout the disk are below the permissible values indicated by the yield and stress-rupture data plotted in figure 6. The compressive tangential stresses at the rim are a direct result of the assumed radial temperature gradient. The values of the radial stresses in figure 8 are somewhat lower than those calculated in reference 7. A principal disadvantage of this disk design is the cost of machining the vane configurations integrally with the disks. This machining, too, was done for reliability in constructing a single research vehicle and eliminating development steps. In the next disk design presented, a more reasonable approach is made to the means by which cooling-air vanes might be constructed for production-model engines.

Split disk with removable vaned insert. - The disk design shown in figure 9 incorporates a removable insert that contains vanes forming the cooling-air passages. The air-passage arrangement is similar to that shown in figure 7, except that the curved inducer vanes have been omitted for simplicity. The vanes could be fabricated from sheet-metal channels welded to a central plate as shown, be cast, or be machined from an integral piece. Any of these methods of fabrication would be easier than that necessary in the disk of figure 7, and it would be possible to use a lighter material like titanium for the insert. As shown in figure 9, the insert is piloted at the outer rim only, since clearance holes are provided in the insert for the bolts tying the forward and rear faces together. The vaned insert could be used either with the forward or rear admission of cooling air. Figure 9 shows its application for forward admission and also points up one of the possible disadvantages of the split-disk design. The cooling-air requirements might be such that for some engine applications the large hole required in the forward disk to provide shaft space would cause excessive tangential stresses at the inner diameter.

Figures 10(a) and (b) show the computed stresses in the forward and rear disks, respectively. Since preliminary calculations indicated that a parallel-sided disk of approximately 1/8-inch thickness would be capable of carrying the load of the vanes, the only dead loads in the stress calculations for the disks were those of the blades and interrupted portions of the disk at the rim between adjacent serrated cut-outs for the blade bases.

The stress levels in this disk are generally higher than those for the disk in figure 7, mainly because of reduced metal thickness. The central hole diameter of 6.4 inches, as compared with 4.0 inches in the case of the disk in figure 7, also contributed to increased stresses in the central region of the forward disk. However, this hole size did not significantly influence the stress values at radii greater than approximately 6.0 inches. This observation can be made by comparing the stresses plotted in figure 10(b), which are for the rear disk having no central hole, with those of figure 10(a). Stresses for radii over 11.5 inches are practically identical for the forward and rear disks. Stress limits have not been exceeded, as can be noted by comparison of equivalent stresses with the yield and stress-rupture data plotted in figure 6. The design shown in figure 9 can, therefore, be considered to have conservative stresses, since frequently yield stresses have been exceeded in central and rim regions of disks relying on plastic flow to readjust the stresses.

Split disk with narrow rims for plate construction. - The main objective of the design shown in figure 11 was to reduce to a minimum the thickness required in the rim and hub regions of the disks, so that plate stock could readily be used in preference to forgings. Turning disks from plate should favorably affect producibility, even though requirements

for machining will not be significantly different from those for contoured forgings. In order to keep the average stresses in the blade-root fastenings to levels comparable with those in which the disk rim thickness is equal to the length of blade base, the number of serrations in the blade root was increased from two to six (see fig. 5(c)). With this type of narrow-rim design, the blade base must be made rigid enough to distribute the centrifugal blade loading to the two rims. For this design, some means of sealing is required between the edges of the base platforms to prevent excess loss of cooling air. Such sealing could be effected by driving soft metal wedges between the rim of the disks and the lower surface of the blade-base platform. Those wedges would be forced into the openings between the base platforms under the action of centrifugal forces.

The cooling-air vanes (fig. 11) may be stamped from two sheet-metal plates and spot-welded to the disks. The vanes are so formed that one cooling-air passage supplies three blades. Experimental data must be obtained on such a configuration to determine if one coolant passage could be developed that will supply three blades with equal amounts of cooling air. Tie-bolts are provided at two radii and are incased by bushings that act as spacers between the disks and reinforce the tie-bolts against bending due to centrifugal or gyroscopic forces.

The stresses plotted in figure 12 are for the rear disk of the plate design of figure 11. The stress values are appreciably higher than for the previous two disks. The use of thinner metal at the central hole and the requirement that the disk carry the dead weight of the vane configuration between the disks are jointly responsible for these increased stresses; however, the stresses are within acceptable limits. Elastic stresses are exceeded only in the region between radii of 2.0 and 2.1 inches, as may be noted by reference to the data in figure 6, which were obtained from heat-treated bar stock. The assumption was made here that these properties (fig. 6) can be closely approached when plate stock of appropriate thickness is used. The type of sheet-metal vane configuration used in the disk of figure 9 could be adapted to the design of figure 11 and would result in some stress reduction.

It is emphasized, however, that the stresses reported herein are due only to centrifugal forces and thermal effects; and, should consideration be given to the use of a split-type disk (particularly plate construction) for production engines, careful attention should be given to the stiffness of the shaft connection for resisting maneuvering loads.

Single Disk With Cooling-Air Shroud

The single-disk designs have the advantage of more effectively using the disk material. All the material is attached to the shaft so that it is all used in resisting the gyroscopic couples set up during maneuvering.

The axial variation in radial temperature gradient is less of a problem in the single disk as compared with multiple disks, because all forces resulting from differential thermal elongation are distributed through successive radial planes at all radii. In the case of multiple disks, all forces resulting from differential thermal deformation must be accommodated by additional rim loadings in the cooler disk. The single disk is adaptable to either forward- or rear-face admission of cooling air. The cooling-air passages, however, for a single-disk design are usually more complicated than those for the split-type disk, with the result of greater cooling-air pressure drops. Also, in some cases, it is more difficult to achieve good distribution of the cooling air along the axial length of the blade.

The effect of the shrouds on the centrifugal disk stresses presented is negligible because of their relatively light weight and the fact that the shrouds are self-supporting to a large extent. No attempts were made to compute thermal stresses that may result because of differential expansion between the shrouds and the disks.

Single disk with cooling-air shroud on forward face. - Figure 13 introduces the first of the shrouded single-disk designs. The shroud is attached to the forward face of the disk by means of T-section sheet-metal strips which also act as vanes for the cooling air. These sheet-metal strips are welded to the disk and project through slots in the shroud when it is placed in position on the disk. The clearance between slots and vanes is filled with weld metal, and thus the shroud is fastened to the disk. The shroud is welded to the disk at the outside diameter to seal the joint. Air is introduced into the blade base by openings milled through the disk. The U-shaped cups at the entrance to these openings in the disk rim are intended to improve entrance flow conditions. This design as shown has only one vane for every three blades.

The results of stress computations on this disk are plotted in figure 14. In these calculations the circumferentially discontinuous metal between air entrance holes at the rim was assumed to be dead load. The shrouded single disk of figure 13 was designed with approximately the same amount of metal as in the split disks of figure 9. The results of the stress analysis, plotted in figure 14 for the shrouded disk of figure 13, are not significantly different from those obtained for the split disks. The stresses in the shrouded disk are lower at the center than for the split disks that have large central holes, and higher in this region than the split-disk half without the cooling-air entrance hole. The stresses are somewhat higher in the mid-radius portions of the disk and nearly identical at the rim when compared with the split-type disk. Nowhere in the disk shown in figure 13 are the stresses beyond the yield strength or the 1000-hour stress to rupture, as appropriate (see fig. 6).

The shroud configuration did not lend itself to any straightforward method of stress analysis. An approximation was made by treating the shroud as a series of separate pie-shaped segments supported by the vanes. The calculated stresses on such segments subjected to the pressure loading of the cooling air were not prohibitively high. The calculated stresses in the vanes and welds in withstanding both the pressure loading and centrifugal loading were also acceptable.

Single disk with cooling-air shroud on rear face. - A disk similar to that described by figure 13 is shown in figure 15 with a shroud on the rear face. In this design the cooling air is introduced through a hole in the main turbine shaft, which eliminates the need for a rotating seal in the hot zone of the engine, and cooling-air piping through the congested turbine bearing supports. These advantages also apply to a split-disk design in which air is introduced through the shaft; however, no layout of such an arrangement is included, as it is a reasonably obvious combination of other designs presented. In the shroud design shown in figure 15, the central hole is much smaller than that of figure 13, and the center region of the shroud is reinforced to some extent by the bullet that extends into the hollow shaft. The main difference in the disk configuration occurs in the rim. In this disk an undercut is made beneath the blade base to form a cooling-air entrance passage from the shroud to the blade base. This undercut goes completely through the rim at a constant radius and permits a clearer dictinction between the continuous disk and dead-load regions in the rim than was the case for the disk shown in figure 13. Here again, the vanes are fabricated from T-shaped sheet-metal sections with a cooling-air passage for every blade. Every third vane is extended and curved to provide a favorable angle of attack for the cooling air, in an effort to reduce cooling-air pressure losses. All the vanes are welded to the disk, and the shroud is welded to every third vane. Axial restraint at the rim of the shroud is provided by a snap ring that fits into a circumferential groove. This snap ring also locks the blades in position axially, as the groove it rides in passes alternately through blade base and disk material. The calculated stress levels are substantially the same for both shrouded disks, as may be noted by comparing figures 14 and 16; however, in the disk shown in figure 15 the cooling-air passages within the disk proper run only in the axial direction underneath the blade base. Consequently, in comparing the radial stress values at the rim on the stress curves included, it may be noted that this arrangement results in the lowest unit rim loading of any of the disks presented. The stress analysis of this type disk design is perhaps a degree more reliable than for the disk in figure 13, because the necessary assumptions on load distribution are much more clear-cut. The blade base used in this design is the same as shown in figure 5(a), except for the addition of a lip (fig. 15(a)) under the leading-edge portion of the base to seal the air passage through the disk rim.

DESIGNS FOR AIR-COOLED TURBINE ROTOR INSTALLATION

In order to illustrate some of the typical problems encountered in utilizing an air-cooled turbine rotor design in a turbojet engine, the following three types of engine installation were studied: rear-face entrance with tail-cone cooling-air supply, forward-face entrance with turbine bearing-support cooling-air supply, and turbine-shaft cooling-air supply with rear-face distribution.

Tail-Cone Cooling-Air Supply

The installation of the split-type disk shown in figure 7 with the cooling-air supply ducted through the tail cone is shown in figure 17. Cooling air is bled from the compressor back to the tail cone through exterior ducts. Oval tubes carry it through the struts connecting the inner and outer tail-cone shells. Inside the tail cone, the oval tubes fair together to form a transition to a round tube at the turbine axis. This tube carries the air forward to the entrance hole in the center of the rear disk. A labyrinth seal is used between the rear disk and the stationary tube carrying the cooling air. The portion of the cooling-air tube directly under the seal fingers is supported by two bearings mounted on a spindle attached to the forward disk. A bellows assembly attaches this portion of the tube to that portion which is attached to the tail cone to allow for radial misalinement. A slip fit between the bellows assembly and the rear portion of the tube allows axial motion.

As shown in figure 17, this type of installation is adapted to the split disk with rear admission of cooling air; however, the tail-cone cooling-air supply entrance is equally adaptable to the use of a single disk with a shroud on its rear face. No drawing is included of this design, inasmuch as it comprises only a straightforward variation of the design shown in figure 15 to provide for tail-cone admission of cooling air rather than shaft admission. The induction system shown in figure 17 has an advantage when applying air-cooling to an existing engine, in that major redesign of the turbine shaft or midframe assembly is unnecessary. There are, however, several disadvantages to this general type of installation. The location of the labyrinth seal and the need for spindle bearings are not desirable. With the use of bleed air from the compressor and the additional heating of the cooling air as it passes through the tail cone, commercially available bearings and bearing lubricants are soon temperature-limited. Thus, in an installation requiring high-pressure cooling air from the compressor, either some cooling of the air would be required before it reaches the spindle bearings, or the bearings must be lubricated or cooled by some external means. The loads put on the spindle bearings by thermal distortions in the tail cone and by tail-cone vibration might reduce bearing life considerably. The pressure-loss characteristics of this type of tail-cone induction system are presented in reference 12.

Turbine Bearing-Support Cooling-Air Supply

A single-disk design with an upstream-face shroud installed in an engine is illustrated in figure 18. The cooling air from the compressor is ducted into the turbine bearing support. Passages formed of sheet metal serve the dual purpose of reinforcing the bearing support and carrying the cooling air aft to the turbine disk. Slots in the rear-bearing housing allow the cooling air to pass through that member and into the shroud passages.

The amount of ducting external to the engine was reduced with this design, and, in general, duct lengths were shorter than those for the tail-cone supply design. However, the smooth flow path obtained with the tail-cone supply system is usually impossible when sections of the bearing support and housing are used to duct air to the upstream shroud. The cooling-air seals are better located in this type of installation, and more effective sealing is possible than in the first type of installation.

Turbine-Shaft Cooling-Air Supply

A single-disk design with downstream-face shroud and with cooling air supplied through the turbine shaft is presented in figure 19. The turbine rotor utilized is similar to that shown in figure 15. In this design, the cooling air was bled radially inward through the rim in the compressor rotor, down between the compressor disks, and into the forward end of the hollow turbine shaft through holes dispersed both axially and angularly in the shafting. The air flows through the shaft to the rear-face shroud and out to the air-cooled blades. In this arrangement, the entire cooling-air induction system is within the engine rotor, and the problems of sealing cooling air between stationary and rotating parts are eliminated. An alternate method consists in bleeding at the outside diameter of the compressor and then ducting the cooling air to the front of the engine, where it enters the hollow compressor shaft. Controlling the amount of air bled at various engine operating conditions might prove to be more difficult with the system shown in figure 19 than the method utilizing an external duct, although this latter method requires a longer path for the cooling air and presents more sealing problems.

There is a stress advantage in the rotating members in the installation of figure 19 in that, when a shroud is used, it is not necessary to have a central hole in it. Also, when a split disk with forward entrance of cooling air is used (which, as mentioned earlier, may be adapted to this type of installation), the size of hole required in the forward disk would be less than in the case of the split disk having upstream entrance of cooling air as shown in figure 9.

Instead of a long tie-bolt through the turbine shaft, a special nut, submerged in the forward end of the shaft, is used in the layout shown in figure 19 as a tie to balance compressor and turbine thrust loads.

The most obvious disadvantage to introducing the cooling air through the shaft is the requirement for increased bearing sizes and, accordingly, bearing speeds. The limitation of this effect was checked when the example turbine layout shown in figure 19 was made. It was found that using a bearing DN value of 880,000 allowed sufficient wall space for shafting and a hole size large enough to hold calculated pressure losses in the shaft portion of the coolant-air supply system to about 1 percent of the available pressure for coolant-flow ratios of 0.05. This DN value is well below the upper ranges of current bearing applications.

COMPARISON OF WEIGHTS AND CRITICAL-MATERIAL CONTENTS OF AIR-COOLED AND UNCOOLED TURBINE BLADES AND DISKS

Weight Comparison

All the designs presented herein have been based on computed stresses that are considered conservative. Comparisons are made with an uncooled turbine that does not necessarily represent the limit of development. The weight comparisons that follow are thus intended to apply within the design scope presented, and not as a limiting quantity comparison.

Blades. - A weight comparison between the uncooled production blades and the equivalent untapered- and tapered-shell air-cooled corrugated-insert blades similar to that in figure 1 is presented in table III(a). The weights of the air-cooled blade components, weight of one blade, and total weight of one complete set of blades are tabulated and compared. (The air-cooled blade weights were computed with the blade base of fig. 5(a).) The air-cooled blade set is approximately 22.4 percent lighter when the untapered shell of 0.018-inch thickness is used, and 10.6 percent lighter with the outer blade shell tapered from 0.018-inch thickness at the tip to 0.042-inch thickness at the root. Because of the increased chord, the individual weight of an air-cooled blade is somewhat greater than that of a solid blade, despite its inherently lighter construction; therefore, the saving in weight for a complete blade set was effected by the use of a smaller number of blades.

Disks. - The weights of the production disk and the five air-cooled disks considered are presented in table III(b). It should be noted here that the weights of all the disks presented include only the material beyond a radius of 2.18 inches, which is the approximate shaft radius, since the method of shaft attachment will be dependent somewhat upon the engine configuration. For a given application, the calculated weights

of single-disk turbine wheels are not significantly different from those of split-disk wheels. The heavier weight (21 to 28 lb) of the split disks reported here is principally the result of employing more extensive vane configurations in the split disks. Except for the disk of figure 7, which was designed primarily as a heat-transfer research turbine, all the disk designs compared favorably in weight with the production disk. From purely geometric considerations, however, the uncooled disks have a basic advantage, since they are free of any additional dead loads such as shrouds or vane systems that are necessary in air-cooled designs. In the air-cooled designs, however, the use of the lighter-weight set of air-cooled blades reduces to some extent the imposed rim loadings. In addition, for a given gas temperature, the reduced rim temperatures that will result from cooling permit higher stress levels. Based solely on the stress analysis of the air-cooled disks presented herein, it appears that substantial reductions in disk weights as well as weights of disk and blade assemblies can be made. Table III(c) indicates a weight saving of 6.2 to 22.2 percent compared with the equivalent production uncooled wheel.

Critical-Material Comparison

The reduction of metal operating temperature through the use of air-cooling permitted the use of low-alloy steels, and thus effected a large reduction in critical-material content in the turbine. The critical-material (columbium, cobalt, tungsten, chromium, molybdenum, nickel, and vanadium) contents in finished parts, blades and disks, are compared in table IV for air-cooled and equivalent uncooled parts. The comparison was based on using Timken 17-22A(S) in all the air-cooled parts, S-816 for the solid blades, and a combination of Timken 16-25-6 for the rim and SAE 4340 for the hub section of the uncooled disk. The nominal chemical composition of these materials is also presented in table IV. The results of this comparison indicated that all the cobalt, columbium, and tungsten were eliminated and that an average over-all saving in critical material amounted to approximately 57 pounds or 93 percent for a set of air-cooled blades and a typical air-cooled disk.

SUMMARY OF DESIGN ANALYSIS

The general conclusions of the design studies of various types of air-cooled turbine disk and engine installation, all of which utilized the corrugated-insert air-cooled blade, are summarized as follows:

1. The use of air-cooled turbine blades such as the corrugated-insert type does not require extensive alterations to present engine design concepts, and, depending on the particular requirements of each engine application, there are several disk configurations and methods of introducing the cooling air that are worthy of consideration.

2. There is an inherent advantage of the split-type disks, in that, because of the symmetry of the cooling-air passages between the split disks, it is usually easier to arrange for uniform cooling-air distribution to all regions within a particular blade. The disadvantages of the split-type disk are that: (a) roughly one-half of the disk material used to carry blade loading has no direct connection with the shaft, and thus the shaft connection is inherently weak in resisting the gyroscopic couples set up during high-speed maneuvers and (b) dissimilar radial temperature gradients in the split disks are also considered a more serious problem than an axial variation in radial temperature gradient within a single disk.

3. The single disk with the lighweight cooling-air shroud is more adaptable to making a strong connection to the turbine shaft for resisting the gyroscopic forces from flight maneuvers. All the disk material used to carry blade loading is one homogeneous piece, and axial temperature gradients cause lower thermal stresses. For a given application, the calculated weights of single-disk turbine wheels are not significantly different from those of split-disk wheels. The heavier weight (21 to 28 lb) of the split disks reported here is principally the result of employing more extensive vane configurations in the split disks. The only disadvantage noted for the single disks is the awkward geometry in providing cooling-air passages from an exterior shroud into the blades.

4. A complete set of tapered-shell corrugated-insert air-cooled blades weighed approximately 10 percent less than an equivalent set of solid blades. The disk configurations, with the exception of that in figure 7, were lighter than the production disk, and thus a complete set of blades and disks was 6.2 to 22.2 percent lighter than that with the equivalent uncooled wheel.

5. The use of all cobalt, columbium, and tungsten was eliminated; and the reduction in the total quantity of critical materials (columbium, cobalt, tungsten, chromium, molybdenum, nickel, and vanadium) required to construct a single representative turbine disk and blade assembly for the operating conditions investigated herein amounted to approximately 57 pounds. This value equals a reduction of approximately 93 percent of the critical materials currently present in uncooled turbine rotor designs.

Lewis Flight Propulsion Laboratory
National Advisory Committee for Aeronautics
Cleveland, Ohio, April 28, 1953

REFERENCES

1. Bartoo, Edward R., and Clure, John L.: Experimental Investigation of Air-Cooled Turbine Blades in Turbojet Engine. XII - Cooling Effectiveness of a Blade with an Insert and with Fins Made of a Continuous Corrugated Sheet. NACA RM E52F24, 1952.

2. Ziemer, Robert R., and Slone, Henry O.: Analytical Procedures for Rapid Selection of Coolant Passage Configurations for Air-Cooled Turbine Rotor Blades and for Evaluation of Heat-Transfer, Strength, and Pressure-Loss Characteristics. NACA RM E52G18, 1952.

3. Esgar, Jack B., and Clure, John L.: Experimental Investigation of Air-Cooled Turbine Blades in Turbojet Engine. X - Endurance Evaluation of Several Tube-Filled Rotor Blades. NACA RM E52B13, 1952.

4. Cochran, Reeves P., Stepka, Francis S., and Krasner, Morton H.: Experimental Investigation of Air-Cooled Turbine Blades in Turbojet Engine. XI - Internal-Strut-Supported Rotor Blade. NACA RM E52C21, 1952.

5. Schramm, Wilson B., and Ziemer, Robert R.: Investigations of Air-Cooled Turbine Rotors for Turbojet Engines. I - Experimental Disk Temperature Distribution in Modified J33 Split-Disk Rotor at Speeds up to 6000 RPM. NACA RM E51I11, 1952.

6. Nachtigall, Alfred J., Zalabak, Charles F., and Ziemer, Robert R.: Investigations of Air-Cooled Turbine Rotors for Turbojet Engines. III - Experimental Cooling-Air Impeller Performance and Turbine Rotor Temperatures in Modified J33 Split-Disk Rotor up to Speeds of 10,000 RPM. NACA RM E52C12, 1952.

7. Kemp, Richard H., and Moseson, Merland L.: Investigations of Air-Cooled Turbine Rotors for Turbojet Engines. II - Mechanical Design, Stress Analysis, and Burst Test of Modified J33 Split-Disk Rotor. NACA RM E51J03, 1952.

8. Heaton, Thomas R., Slivka, William R., and Westra, Leonard F.: Cold-Air Investigation of a Turbine with Nontwisted Rotor Blades Suitable for Air Cooling. NACA RM E52A25, 1952.

9. Petrick, E. N.: A Survey of German Hollow Turbine Blade Development. Part I - Initial Investigations and Developments. Purdue Univ., Purdue Res. Foundation, pub. by USAF-AMC, Wright-Patterson Air Force Base, Dayton (Ohio), Oct. 1949.

10. Manson, S. S.: Determination of Elastic Stresses in Gas-Turbine Disks. NACA Rep. 871, 1947. (Supersedes NACA TN 1279.)

11. Manson, S. S.: Direct Method of Design and Stress Analysis of Rotating Disks with Temperature Gradient. NACA Rep. 952, 1950. (Supersedes NACA TN 1957.)

12. Smith, Gordon T., and Curren, Arthur N.: Comparison of Pressure-Loss Characteristics of Several Tail-Cone Air-Induction Systems for Air-Cooled Gas-Turbine Rotors. NACA RM E52K07, 1953.

13. Anon.: Timken 17-22A and Other Bolting Steels for High Temperature Applications. Tech. Bull. No. 36, Timken Bolting Steel Data Sheets, Steel and Tube Div., The Timken Roller Bearing Co. (Canton, Ohio), 1949.

14. Brown, W. F., Jr., Jones, M. H., and Newman, D. P.: Influence of Sharp Notches on the Stress-Rupture Characteristics of Several Heat-Resisting Alloys. Preprint No. 76 presented at meeting of A.S.T.M., June 23-27, 1952.

TABLE I. - SPECIFICATIONS FOR AIR-COOLED TURBINE

Engine speed, rpm	8000
Tip diameter of turbine, in.	33.46
Root diameter of turbine, in.	26.71
Turbine-inlet gas temperature, °F	1605
Turbine disk material	Timken 17-22A(S)
Turbine blade material	Timken 17-22A(S)
Maximum rim width of disk, in.	2.36
Airfoil span of turbine rotor blade, in.	3.37
Number of blades in complete rotor	72
Axial chord of rotor blade at root section, in.	2.22

[redacted]

TABLE II. - STRESSES IN CORRUGATED-INSERT AIR-COOLED TURBINE BLADES

Airfoil

Average tensile root stress in untapered shell, psi	25,500
Average tensile root stress in tapered shell, psi	20,600
Reduction in root stress by means of taper, percent	19.2

Shell tensile stress at root when failure of corrugation and insert braze causes all load to be transmitted through shell, psi

Untapered shell	61,800
Tapered shell	33,350

Shear stress in brazed joint between base and airfoil shell, psi

Untapered shell	5,250
Tapered shell	6,560

Base (refer to fig. 5 for section location and type of base)

	Base type					
	Two-serrations		Single lug		Six serrations	
	Tapered shell	Untapered shell	Tapered shell	Untapered shell	Tapered shell	Untapered shell
Approximate tensile stress, psi						
Section M-M	9040	7500	11,280	9500	9040	7500
Section N-N	6890	5980	------	----	[a]5138	[a]4630
Average bearing stress on projected area, psi						
Dimension 'P'	21,500	18,900	32,300	28,000	18,590	16,750
Collapsing load component of centrifugal force, lb	2040	1770	12,400	10,800	------	------
Average shear stress, psi	15,800	13,700	12,400	10,800	13,600	12,260
Angle β, deg	71.68	71.68	45(mean)	45(mean)	71.68	71.68
Blade base weight, lb	0.208	0.208	0.213	0.213	0.261	0.261

[a]Average value for all serrations.

TABLE III. - WEIGHT COMPARISON BETWEEN AIR-COOLED TURBINE ROTOR COMPONENTS AND THEIR EQUIVALENT UNCOOLED TURBINE ROTOR COMPONENTS

(a) Blades

Component	Weight of production blade, lb	Weight of air-cooled noncritical blades, lb		Weight saved compared with solid blades, lb		Weight saved compared with solid blades, percent		Material in production blades	Material in air-cooled noncritical blades
		Untapered shell	Tapered shell	Untapered shell	Tapered shell	Untapered shell	Tapered shell		
One complete airfoil section	0.267	0.210	0.274	0.058	-0.007	21.4	-2.6	S-816	17-22A(S)
Blade airfoil shell		.089	.153						17-22A(S)
Corrugations		.077	.077						17-22A(S)
Insert		.034	.034						17-22A(S)
Insert cap		.002	.002						17-22A(S)
Braze (estimated)		.008	.008						Copper
Blade base	.142	[a].208	[a].208	-.066	-.066	-46.5	-46.5	S-816	17-22A(S)
One complete blade	.409	.418	.482	-.009	-.073	-2.2	-17.9	S-816	17-22A(S)
One complete set of blades[b]	38.8	30.1	34.7	8.7	4.1	22.4	10.6	S-816	17-22A(S)

[a]Two-serration cast base (fig. 5(a)). Single-lug base and six-serration base are 2.4 and 25.5 percent heavier, respectively, than two-serration base.

[b]Ninety-five blades in production turbine; 72 blades in air-cooled turbine.

TABLE III. - WEIGHT COMPARISON BETWEEN AIR-COOLED TURBINE ROTOR COMPONENTS AND THEIR EQUIVALENT UNCOOLED TURBINE ROTOR COMPONENTS - Continued.

(b) Disks

Type of disk	Weight, lb			Weight saved compared with production disk, lb	Weight saved compared with production disk, percent	Material
	Disk proper	Internal vanes or shrouds	Total			
Production (uncooled)			160			16-25-6 & SAE 4340
Split type (fig. 7)		Integral with disks	241	-81	-50.6	17-22A(S)
Split type (fig. 9)	123	20	143	17	10.6	17-22A(S)
Split type (fig. 11)	125	23	148	12	7.5	17.22A(S)
Shrouded single (fig. 13)	111	11	122	38	23.7	17-22A(S)
Shrouded single (fig. 15)	102	18	120	40	25.0	17-22A(S)

TABLE III. - WEIGHT COMPARISON BETWEEN AIR-COOLED TURBINE ROTOR COMPONENTS AND THEIR EQUIVALENT UNCOOLED TURBINE ROTOR COMPONENTS - Concluded.

[Weight of production wheel (95 blades), 198.8 lb]

(c) Disk and blade assemblies

Type of disk	Weight with untapered-shell blades, lb	Weight saved compared with production wheel, lb	Weight saved compared with production wheel, percent	Weight with tapered-shell blades, lb	Weight saved compared with production wheel, lb	Weight saved compared with production wheel, percent
Split type (fig. 7) (base type (b))	271.4	-72.6	-36.5	276.1	-77.3	-38.9
Split type (fig. 9) (base type (a))	173.1	25.7	12.9	177.7	21.1	10.6
Split type (fig. 11) (base type (c))	181.8	17.0	8.5	186.5	12.3	6.2
Shrouded single (fig. 13) (base type (a))	152.1	46.7	23.5	156.7	42.1	21.2
Shrouded single (fig. 15) (base type (a)*)	150.1	48.7	24.5	154.7	44.1	22.2

*Same base with sealing lip added.

TABLE IV. - COMPARISON OF CRITICAL MATERIAL REQUIRED FOR AIR-COOLED TURBINE WHEEL COMPONENTS AND EQUIVALENT UNCOOLED TURBINE WHEEL COMPONENTS

[See table III for materials]

Component	Element weight, lb							Saving of critical material, percent
	Cb	Co	W	Cr	Mo	Ni	V	
Set untapered-shell air-cooled blades[a]				0.38	0.15		0.08	98.3
Set tapered-shell air-cooled blades[a]				.43	.17		.09	98.1
Set equivalent solid blades	1.55	16.30	1.55	7.76	1.55	7.82		
Production disk				7.82	2.87	12.91		
Split-type disk (fig. 7)				3.01	1.21		.60	79.6
Split-type disk (fig. 9)				1.79	.71		.36	88.0
Split-type disk (fig. 11)				1.85	.74		.37	87.4
Shrouded single disk (fig. 13)				1.52	.61		.30	89.7
Shrouded single disk (fig. 15)				1.50	.60		.30	89.8

Chemical composition

Material	C	Mn	P	S	Si	Cr	Mo	V	Ni	Co	W	Cb
17-22A(S)	0.28-0.33	0.45-0.65	0.040 max	0.040 max	0.55-0.75	1.0-1.5	0.40-0.60	0.20-0.30				
SAE 4340	.38-0.43	.60-0.80	.040 max	.040 max	.20-0.35	.7-0.9	.20-0.30		1.65-2.0			
S-816	.40	.50			.50	20.00	4.00		20.17	42.00	4.00	4.00
16-25-6	.08	1.50			.50	16.00	6.00		25.00			

[a]Composition of braze material assumed to be same as that of parent metal.

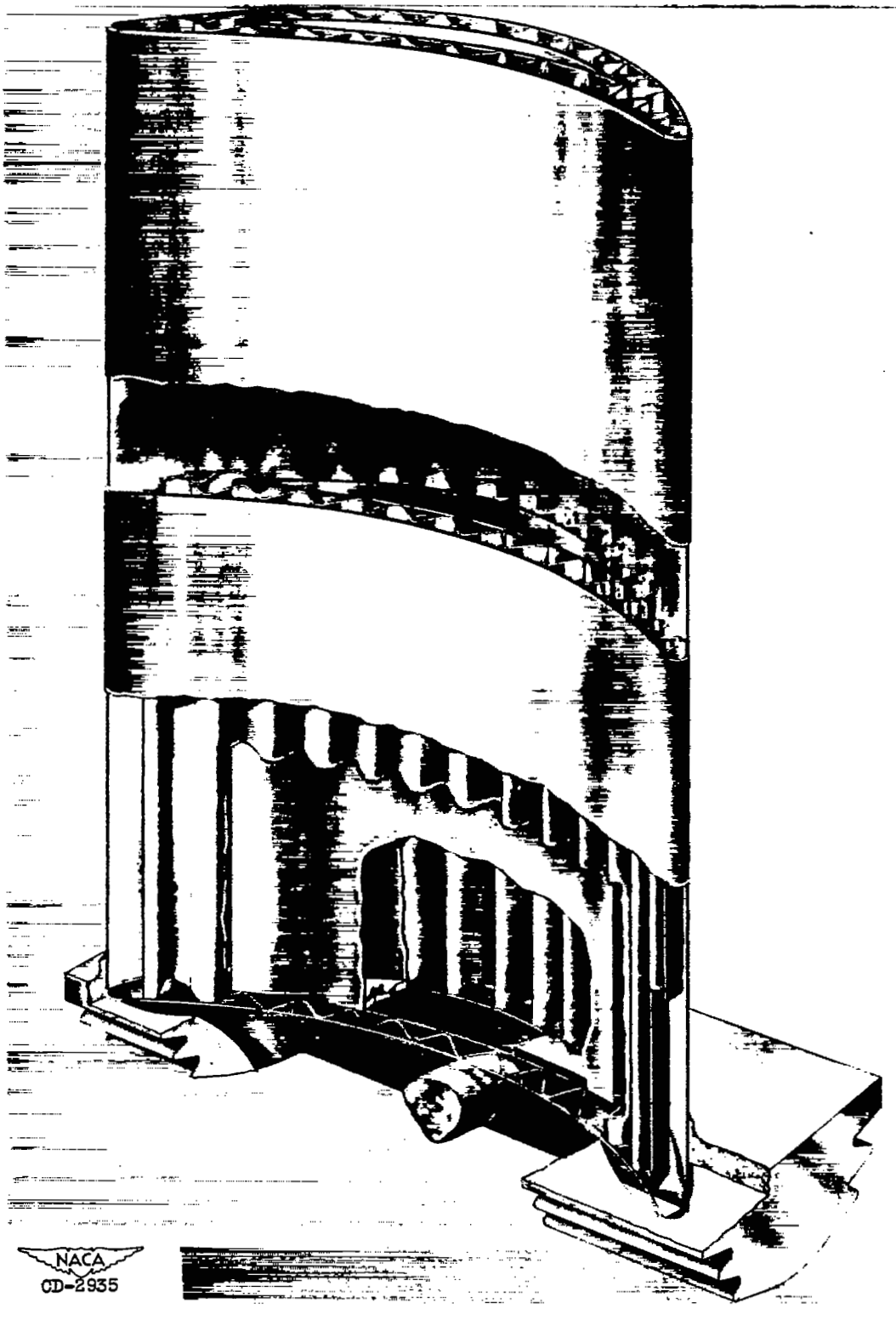

Figure 1. - Isometric sketch of corrugated-insert air-cooled blade.

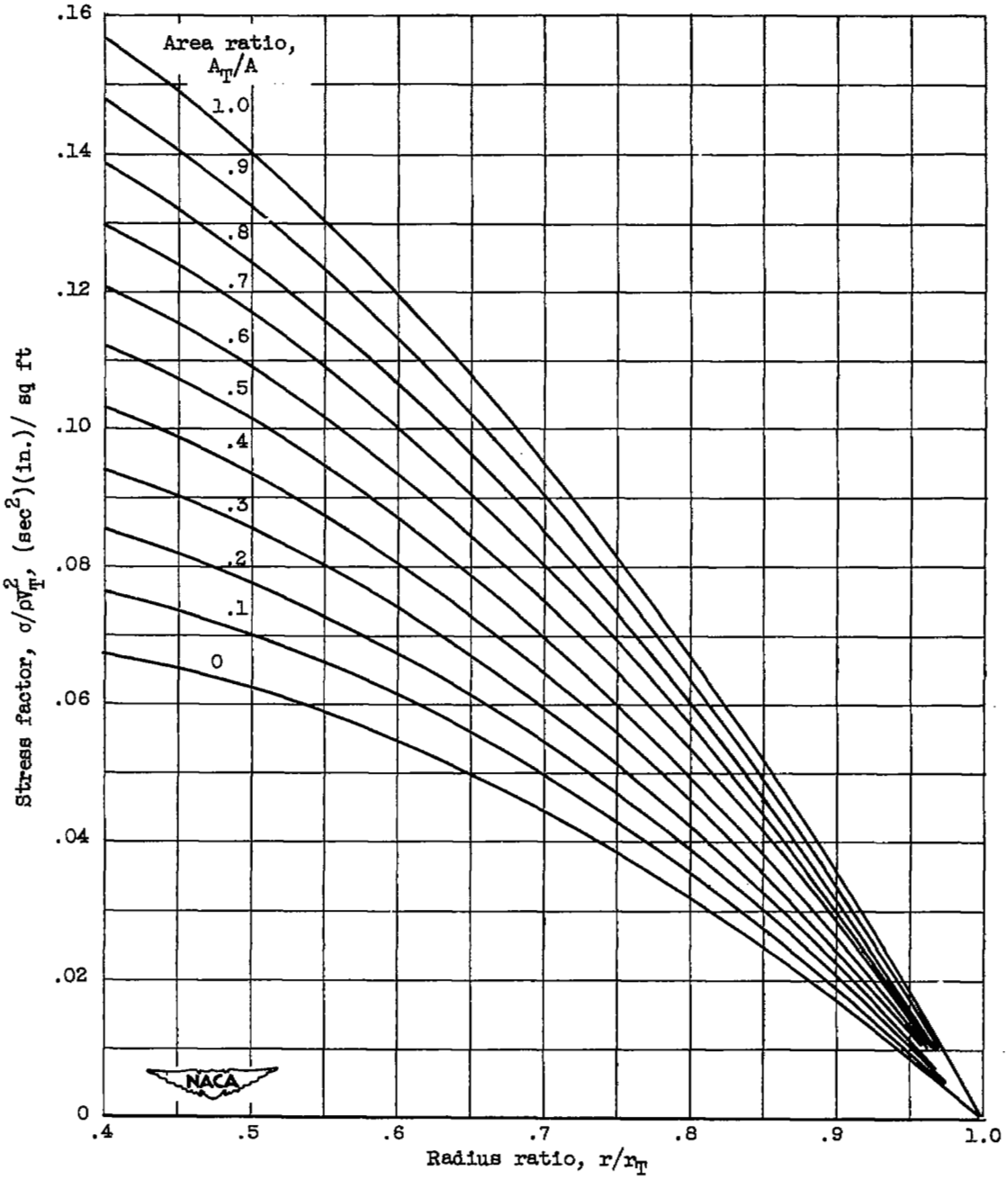

Figure 2. - Curves for calculating stress level at any spanwise position of linearly tapered blades.

[redacted]

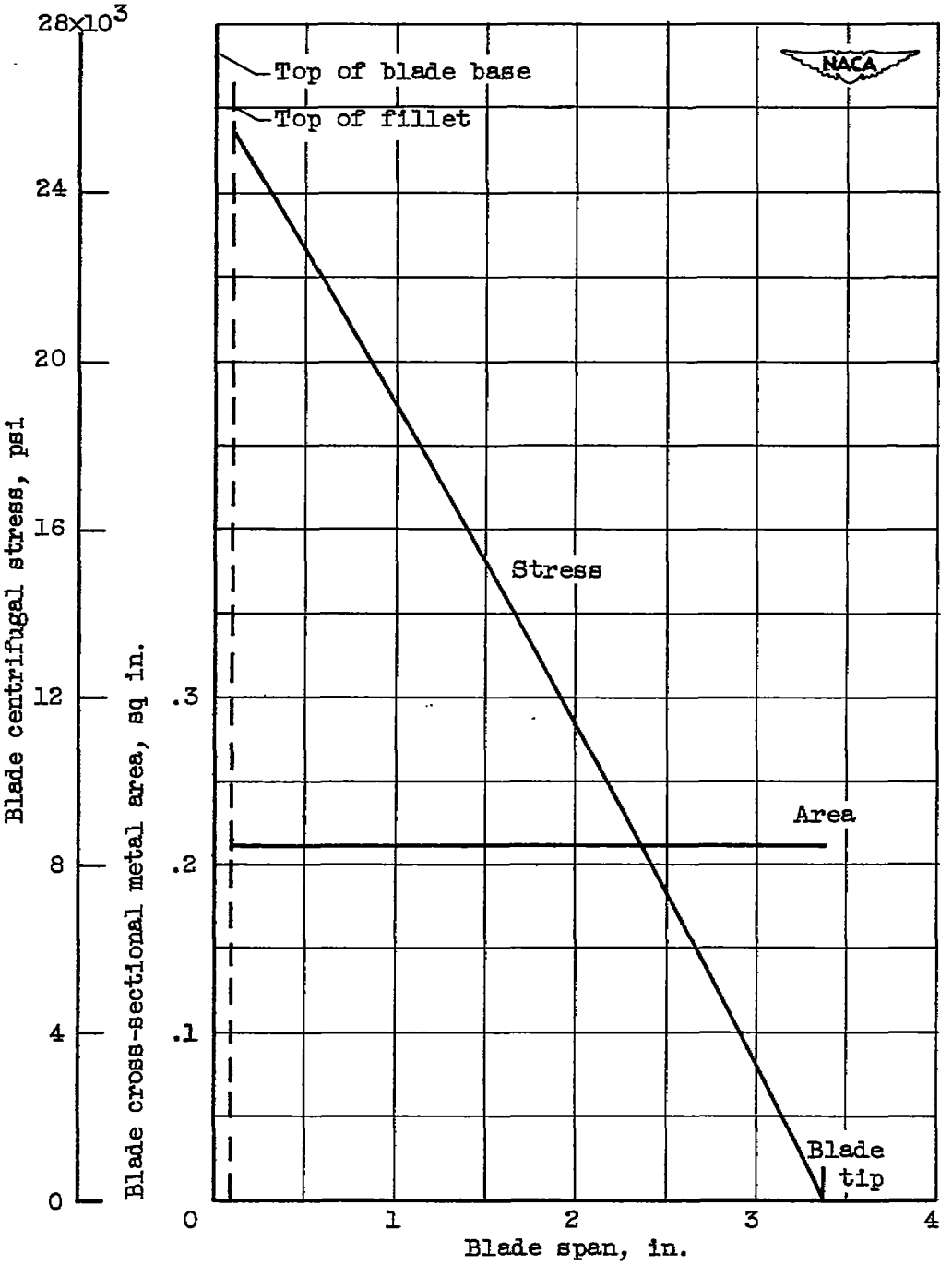

(a) Untapered shell.

Figure 3. - Centrifugal stresses and cross-sectional metal area in corrugated-insert air-cooled blade.

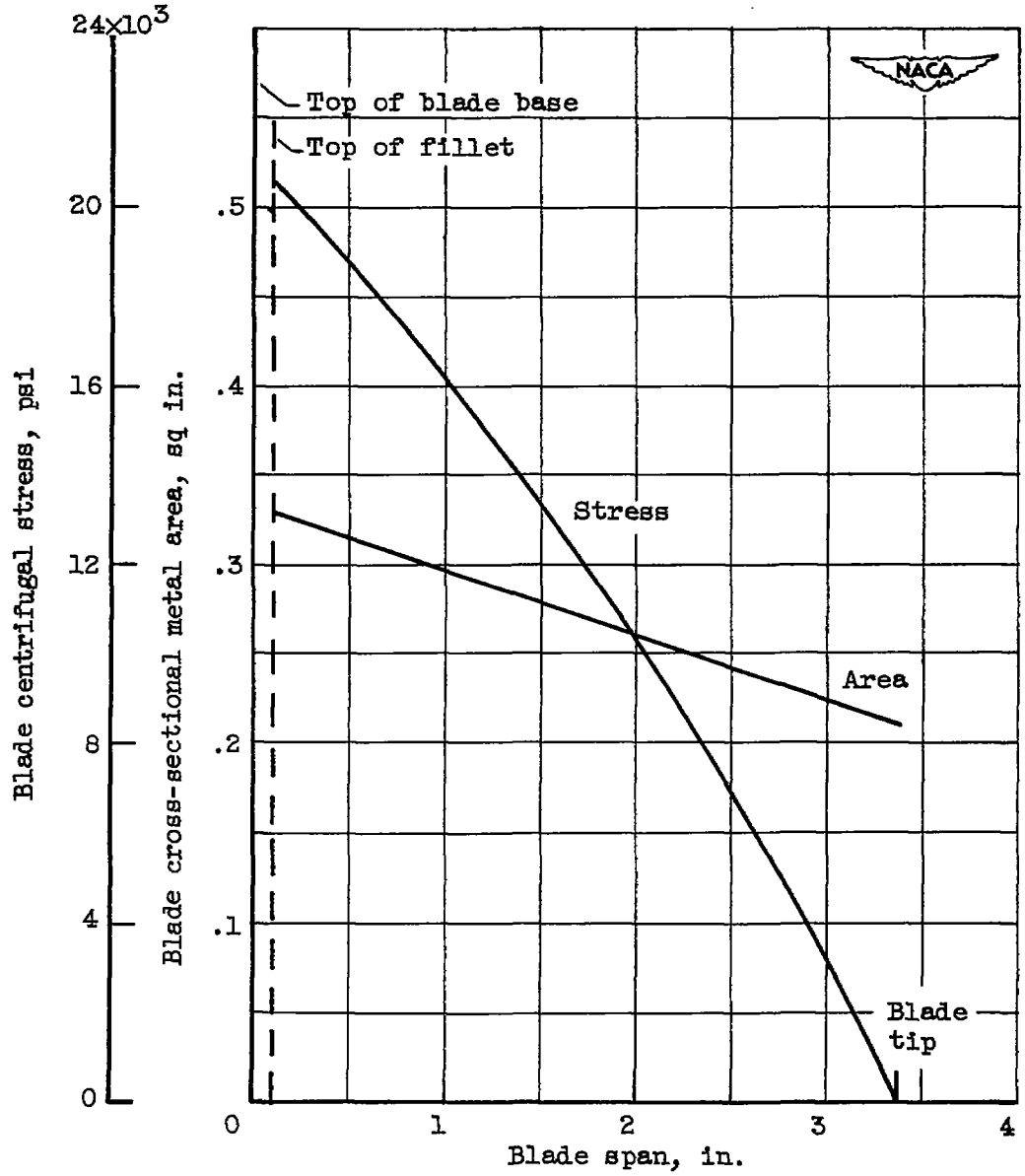

(b) Tapered shell.

Figure 3. - Concluded. Centrifugal stresses and cross-sectional metal area in corrugated-insert air-cooled blade.

[redacted]

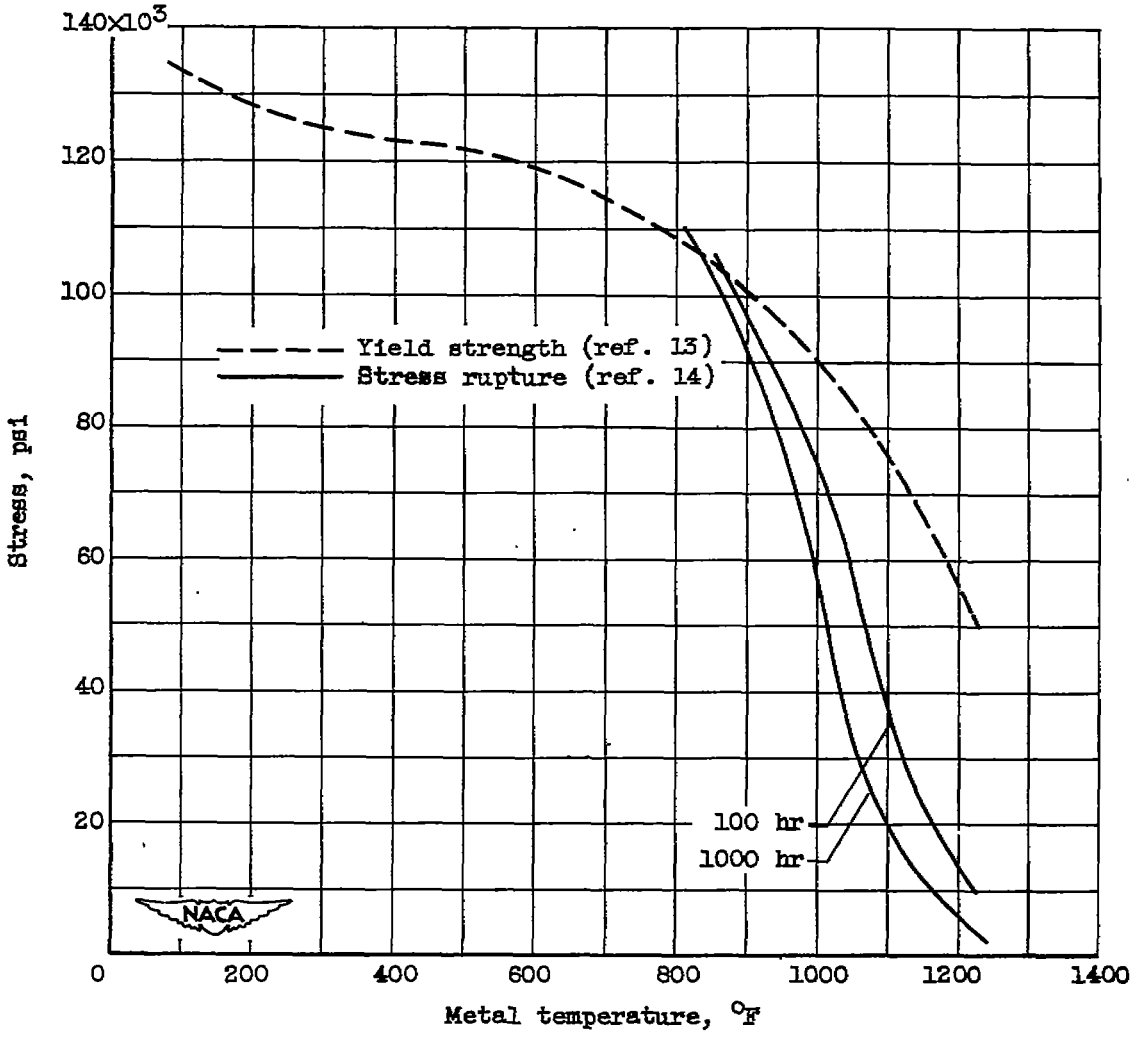

Figure 4. - Yield stress (0.2-percent set) and stress-rupture data for 100 and 1000 hours for Timken 17-22A(S) alloy steel bar stock.

(a) Two-serration cast blade.

(b) Single-lug cast base.

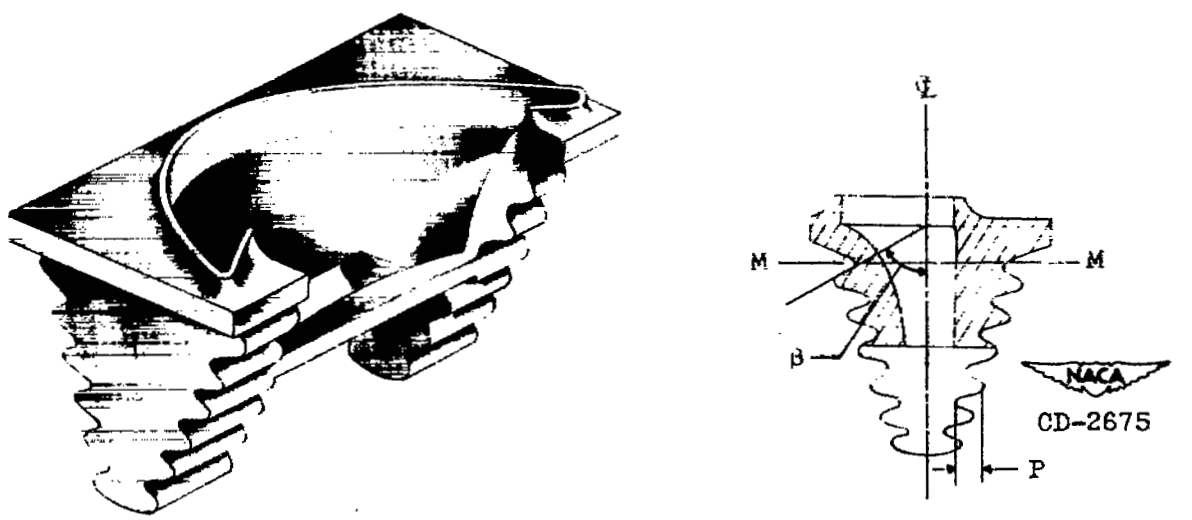

(c) Six-serration cast base.

Figure 5. - Three designs for air-cooled turbine blade base.

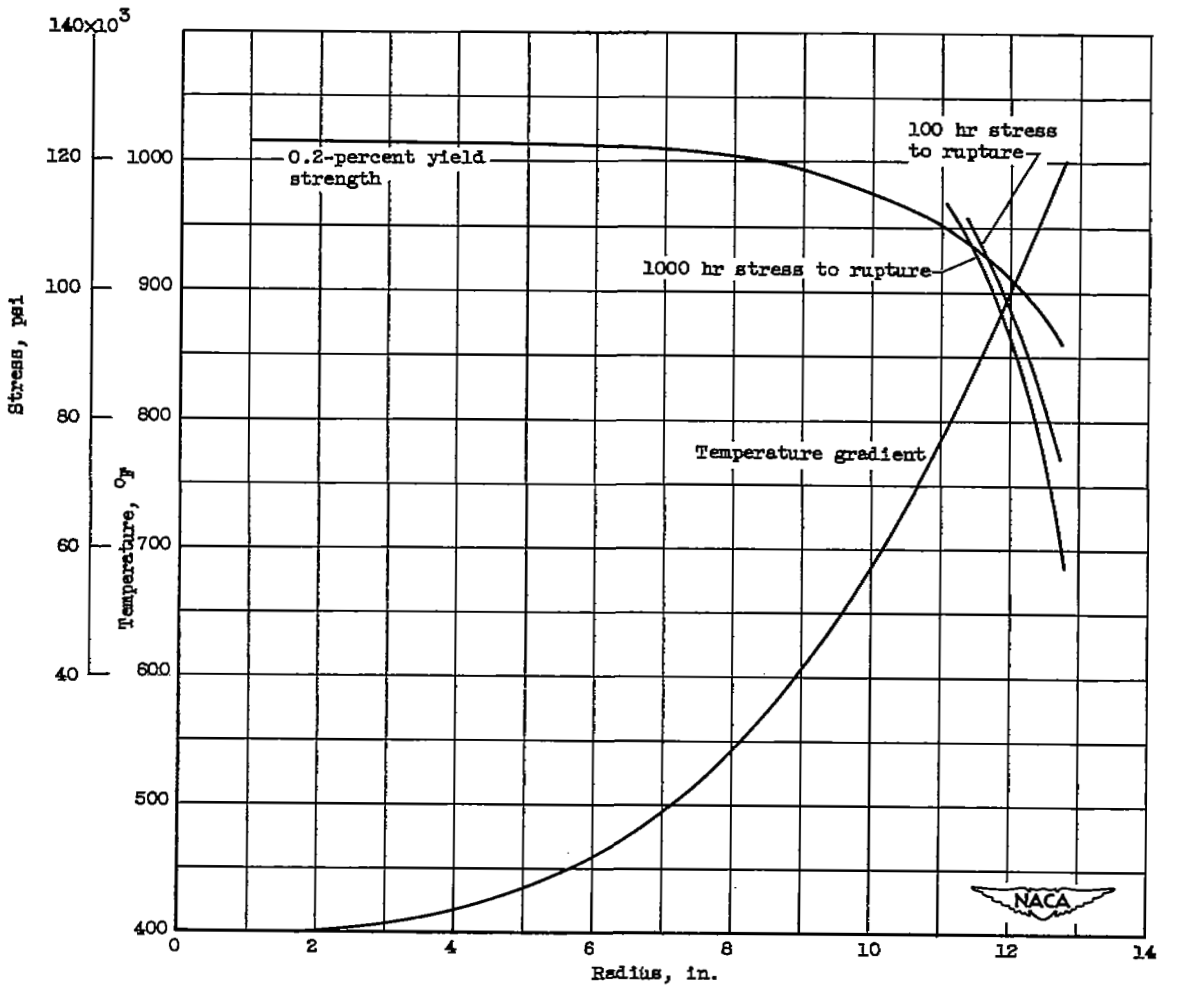

Figure 6. - Radial temperature distribution and corresponding yield strength and stress-to-rupture data for air-cooled disks presented. Timken 17-22A(S) steel.

[redacted]

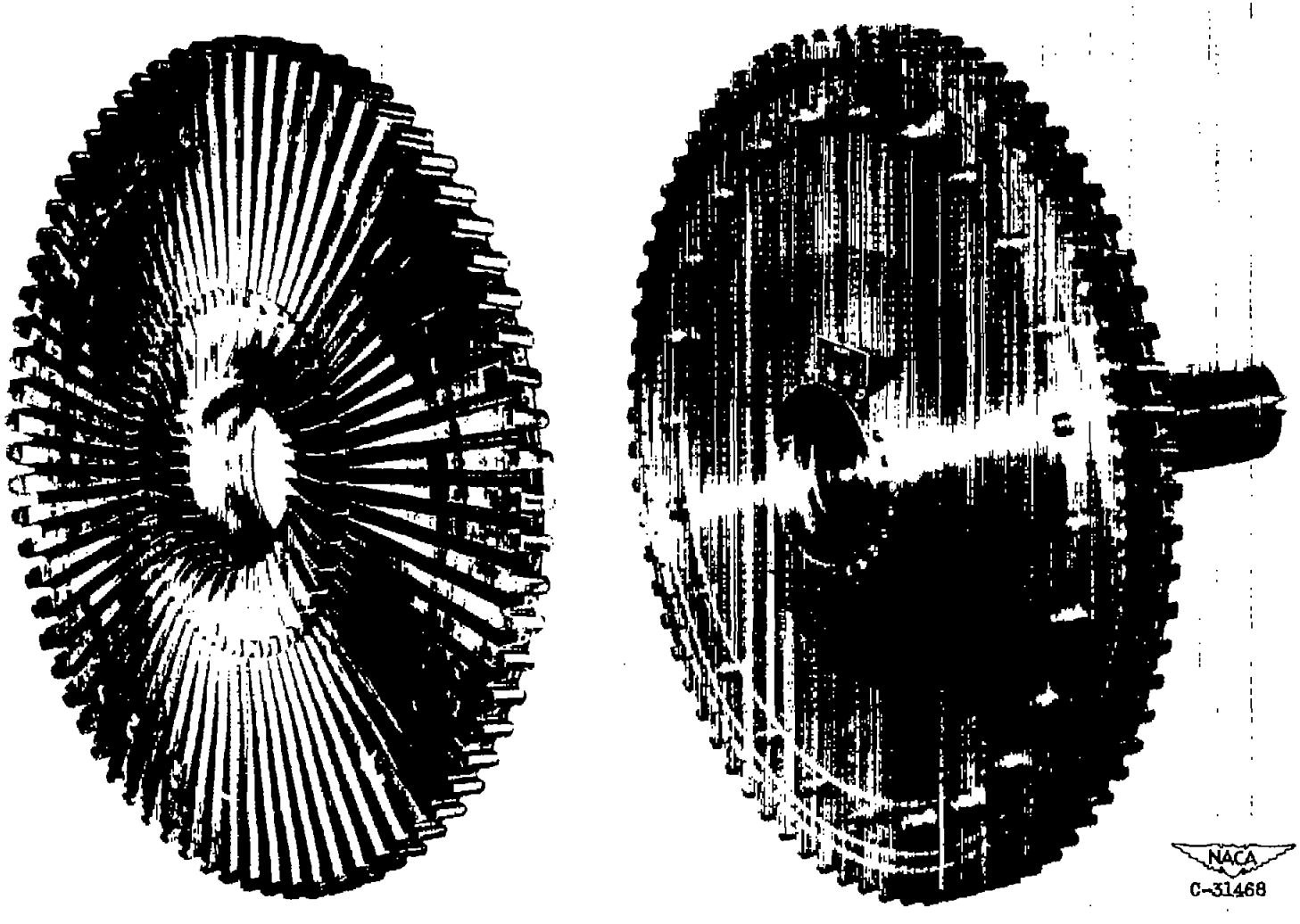

(a) Interior view of rear disk.

(b) Exterior view of assembled disk.

Figure 7. - Split-type air-cooled turbine disk with cooling-air entrance through center of rear disk.

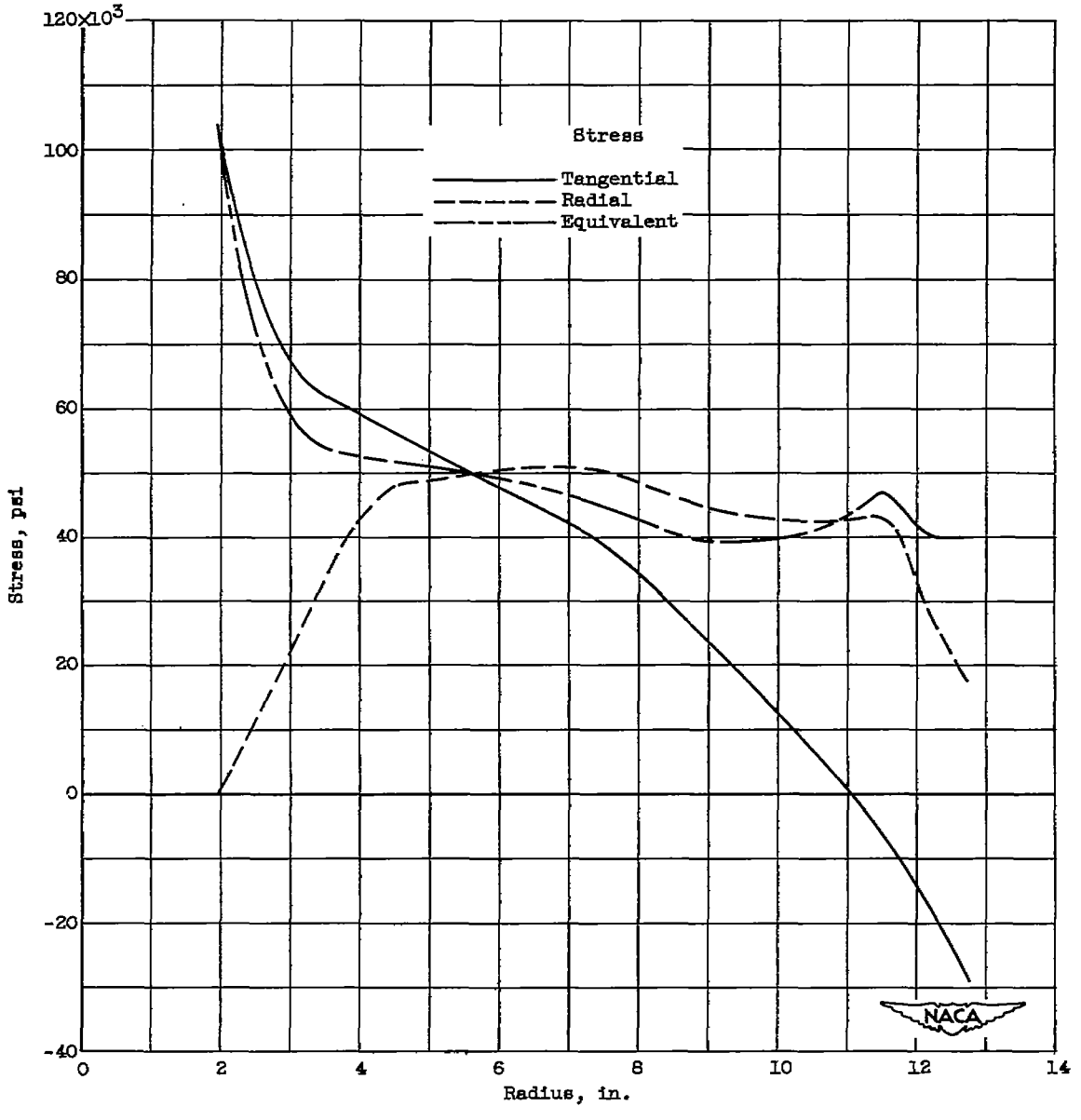

Figure 8. - Stresses in downstream half of split-type air-cooled turbine disk shown in figure 7.

[redacted]

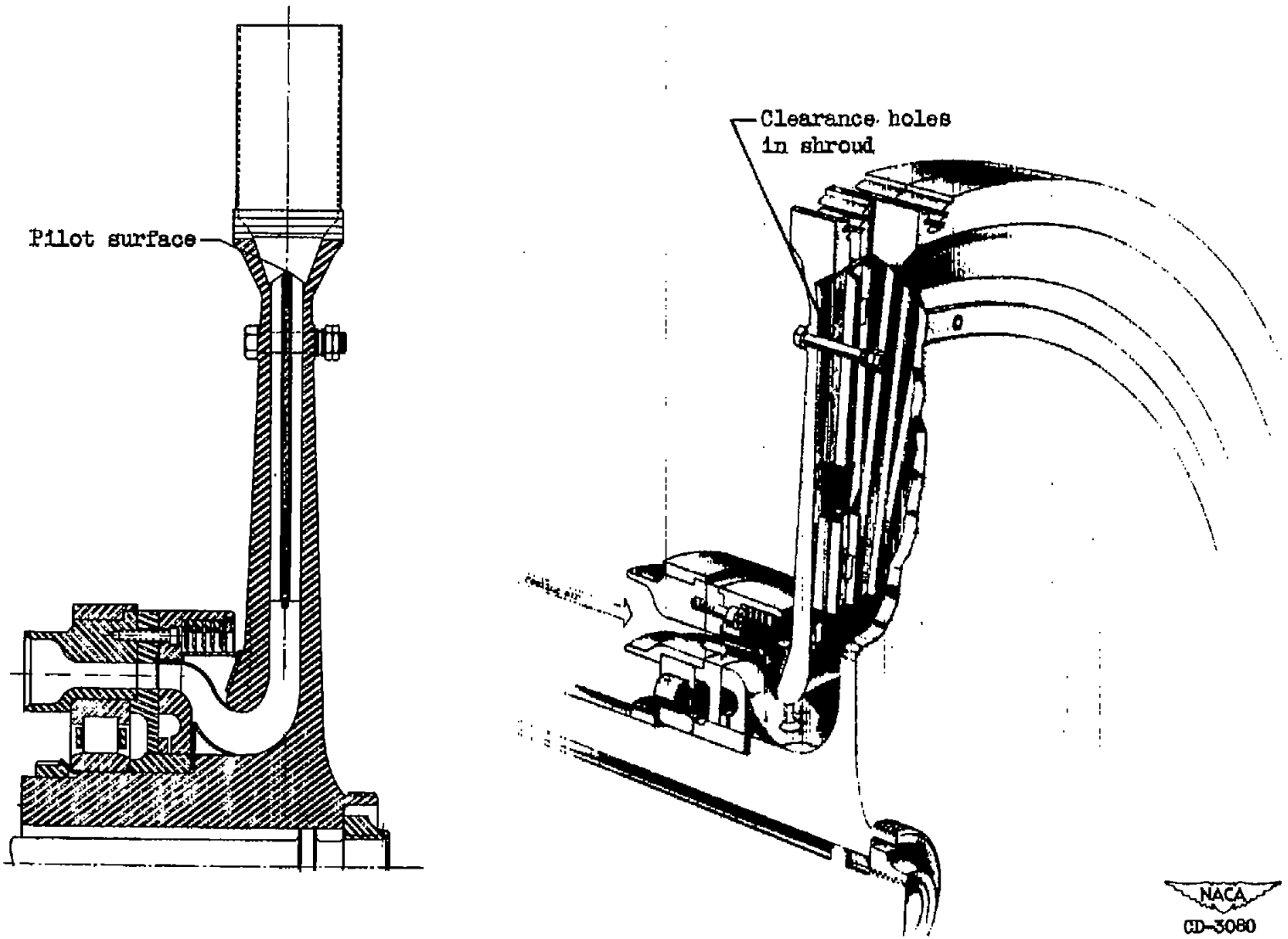

(a) Cross-sectional view.

(b) Isometric view.

Figure 9. - Split-type air-cooled turbine disk with removable vaned insert and cooling-air entrance through central hole in forward disk.

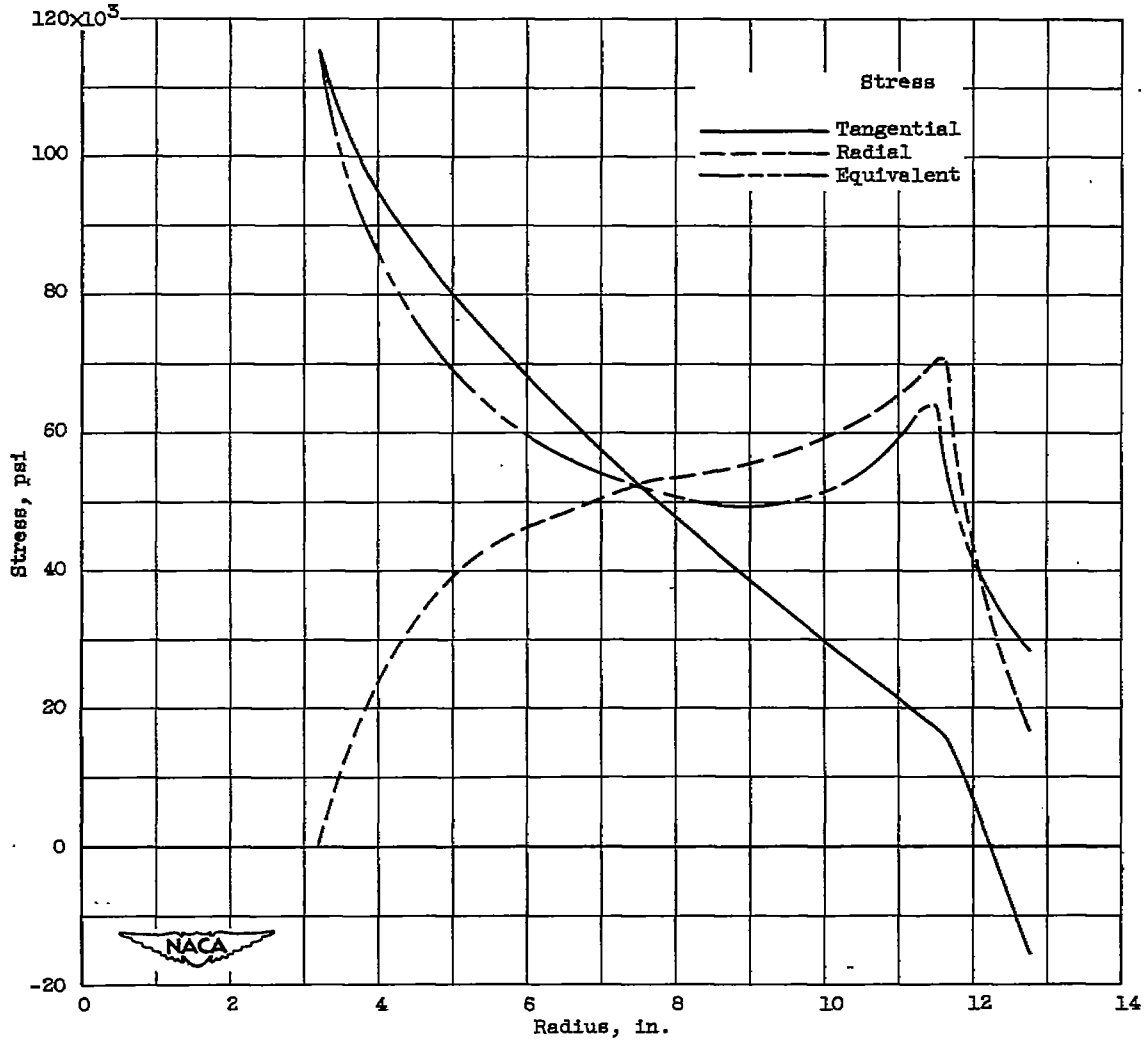

(a) Forward disk.

Figure 10. - Stresses in split-type air-cooled turbine disk shown in figure 9.

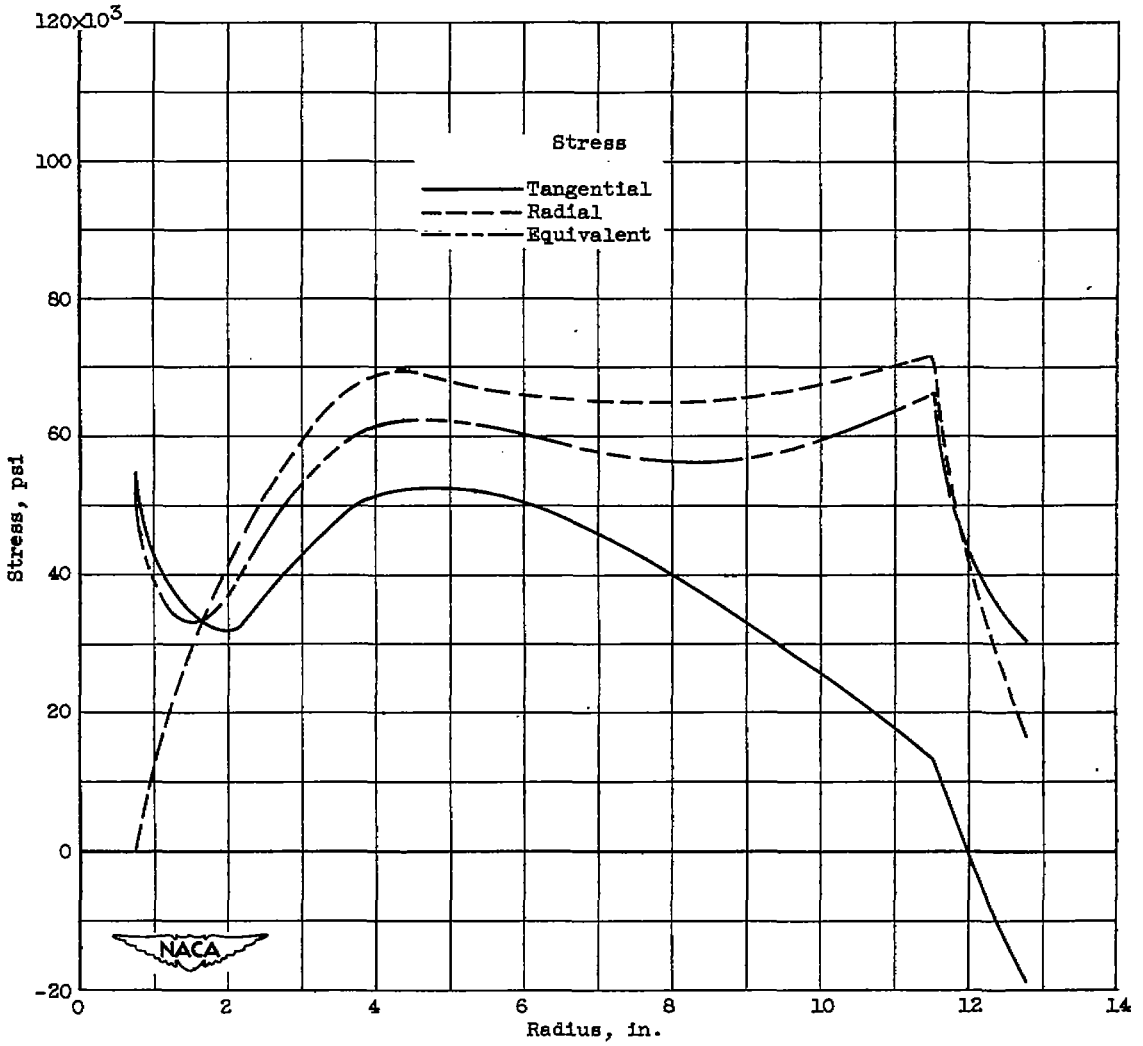

(b) Rear disk.

Figure 10. - Concluded. Stresses in split-type air-cooled turbine disk shown in figure 9.

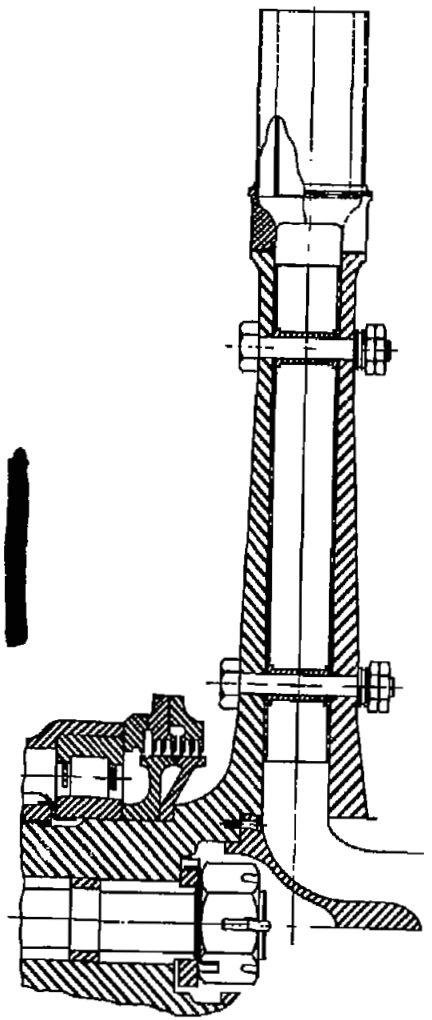

(a) Cross-sectional view.

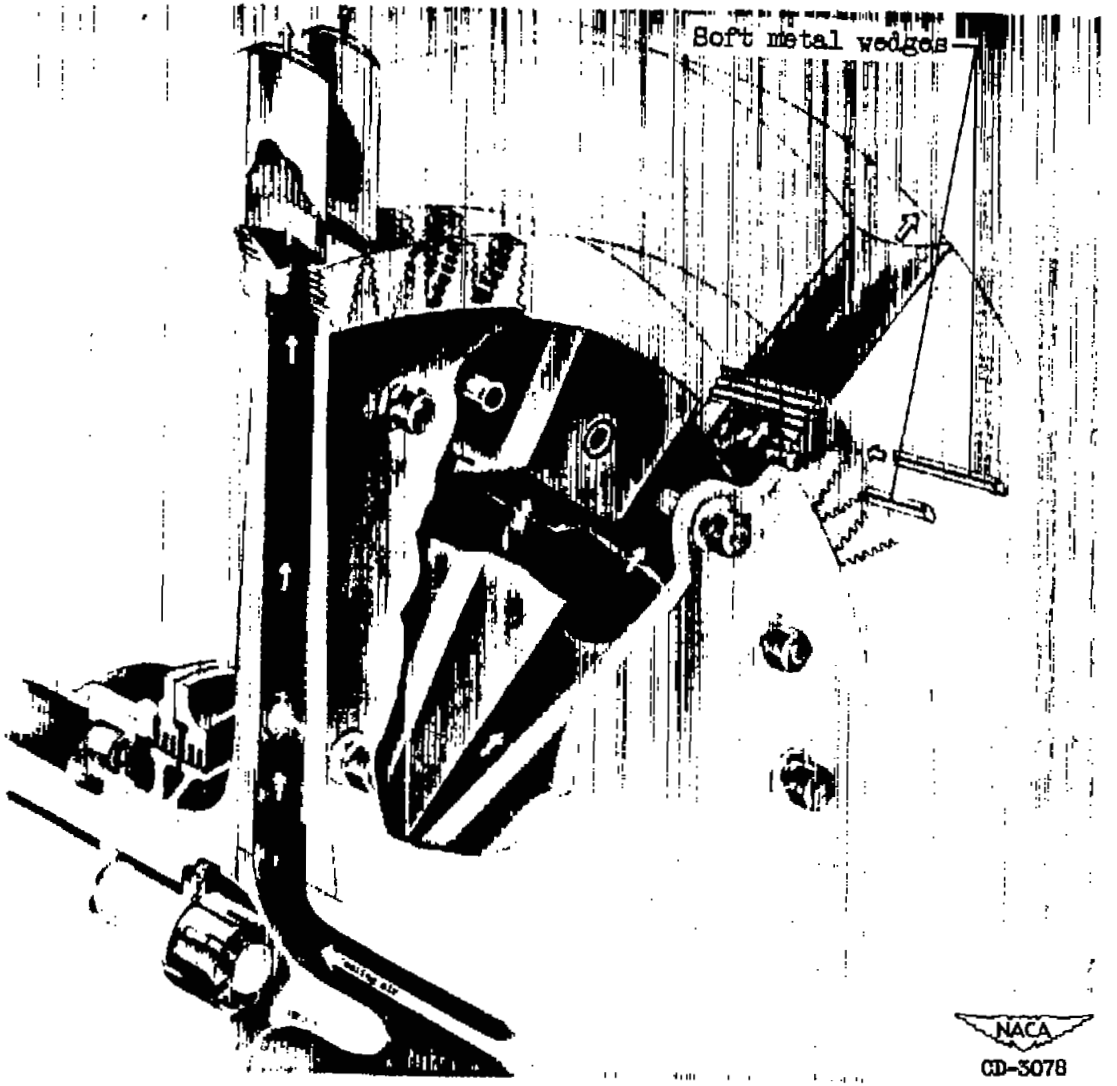

(b) Isometric view.

Figure 11. - Split-type air-cooled turbine disk with narrow rims and stamped metal vanes.

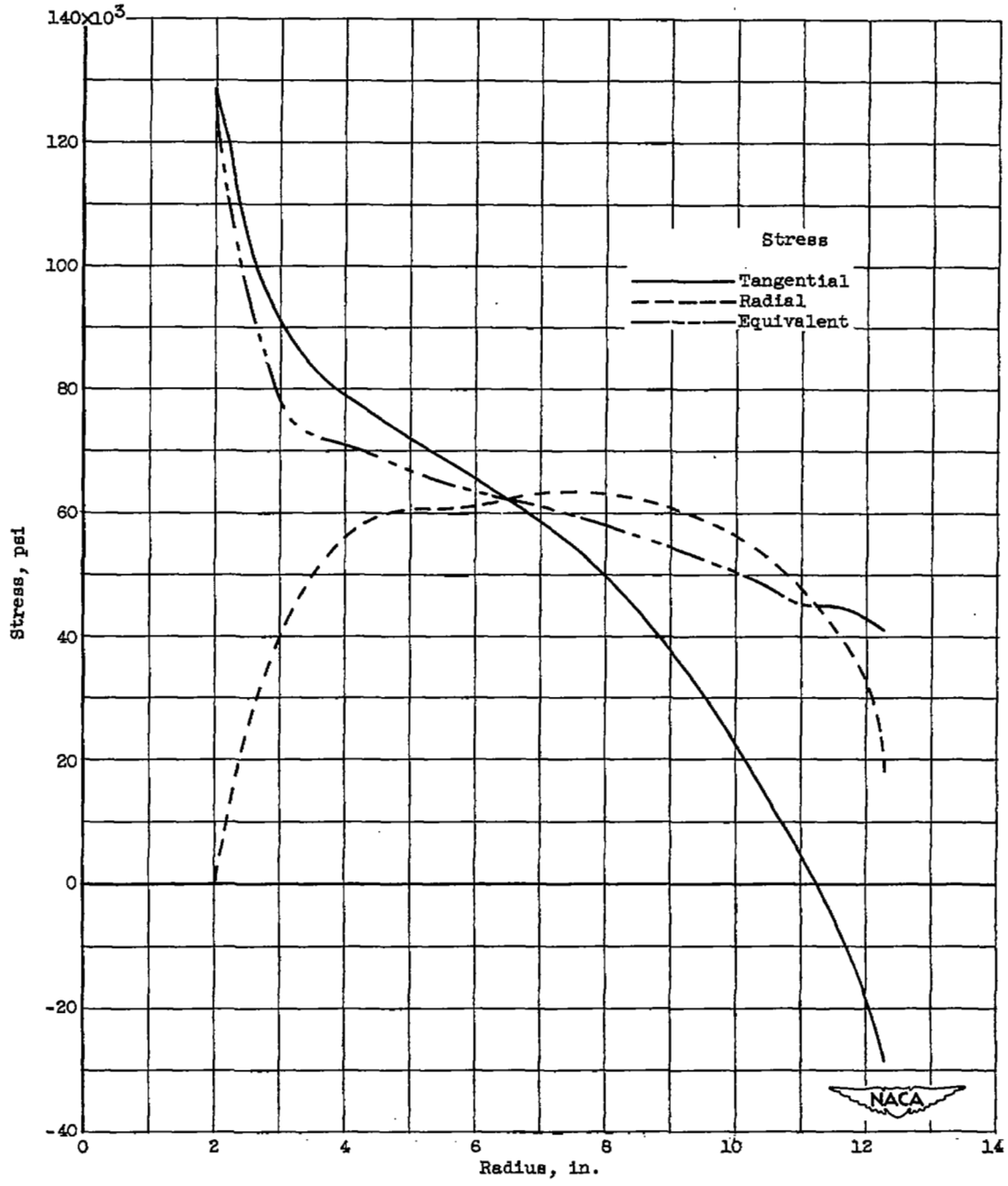

Figure 12. - Stresses in rear half of split-type air-cooled disk shown in figure 11.

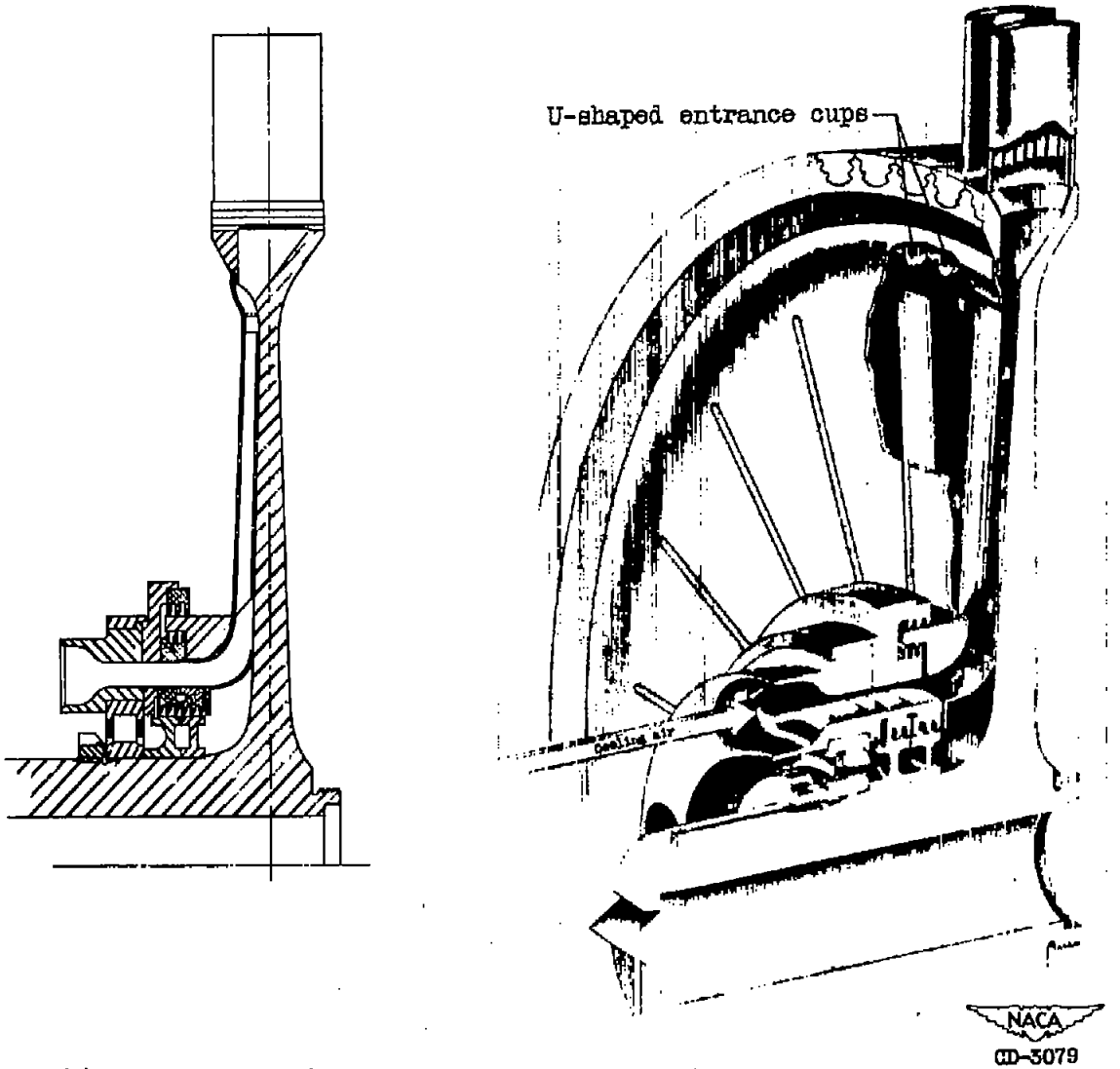

(a) Cross-sectional view.

(b) Isometric view.

Figure 13. - Single-disk air-cooled turbine with cooling-air shroud on forward face.

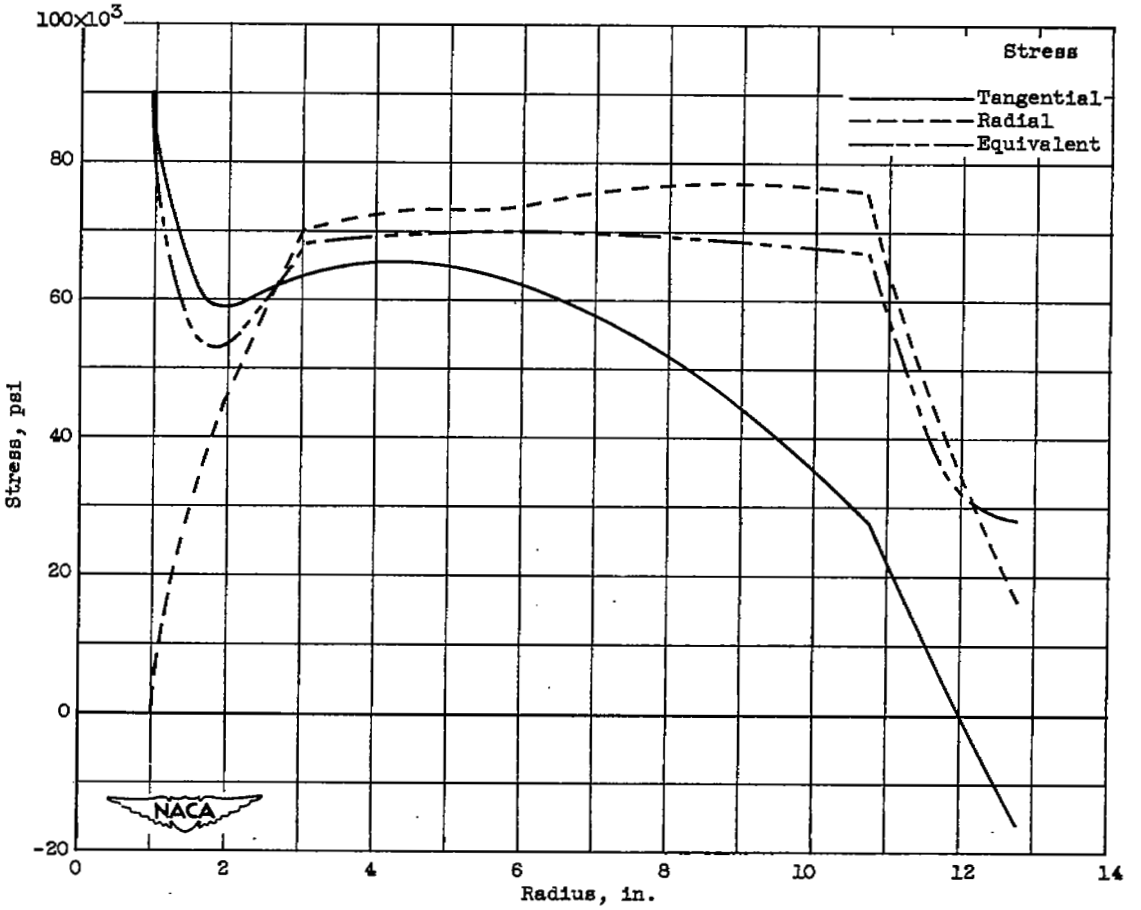

Figure 14. - Stresses in single-disk air-cooled turbine shown in figure 13.

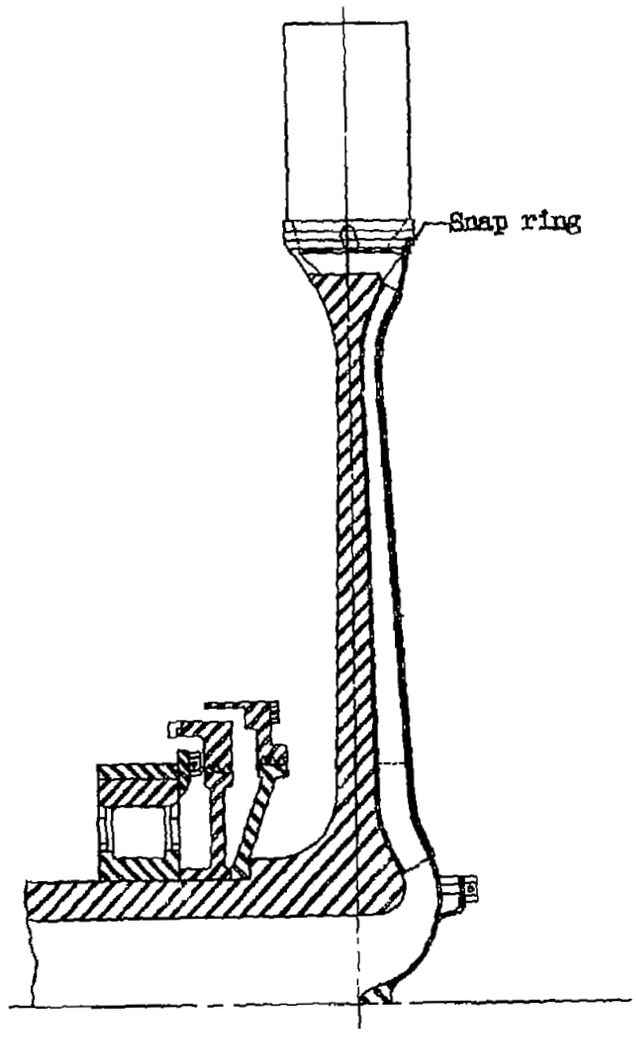

(a) Cross-sectional view.

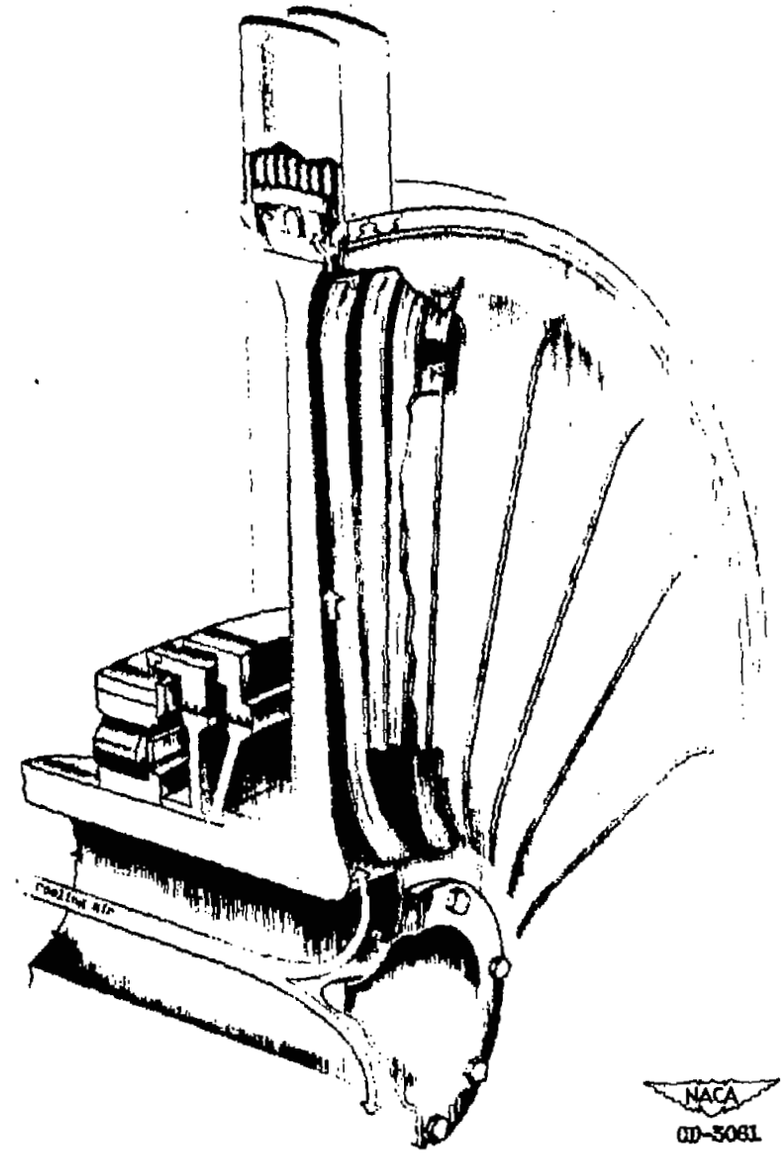

(b) Isometric view.

Figure 15. - Single-disk air-cooled turbine with cooling-air shroud on rear face and central air supply through shaft.

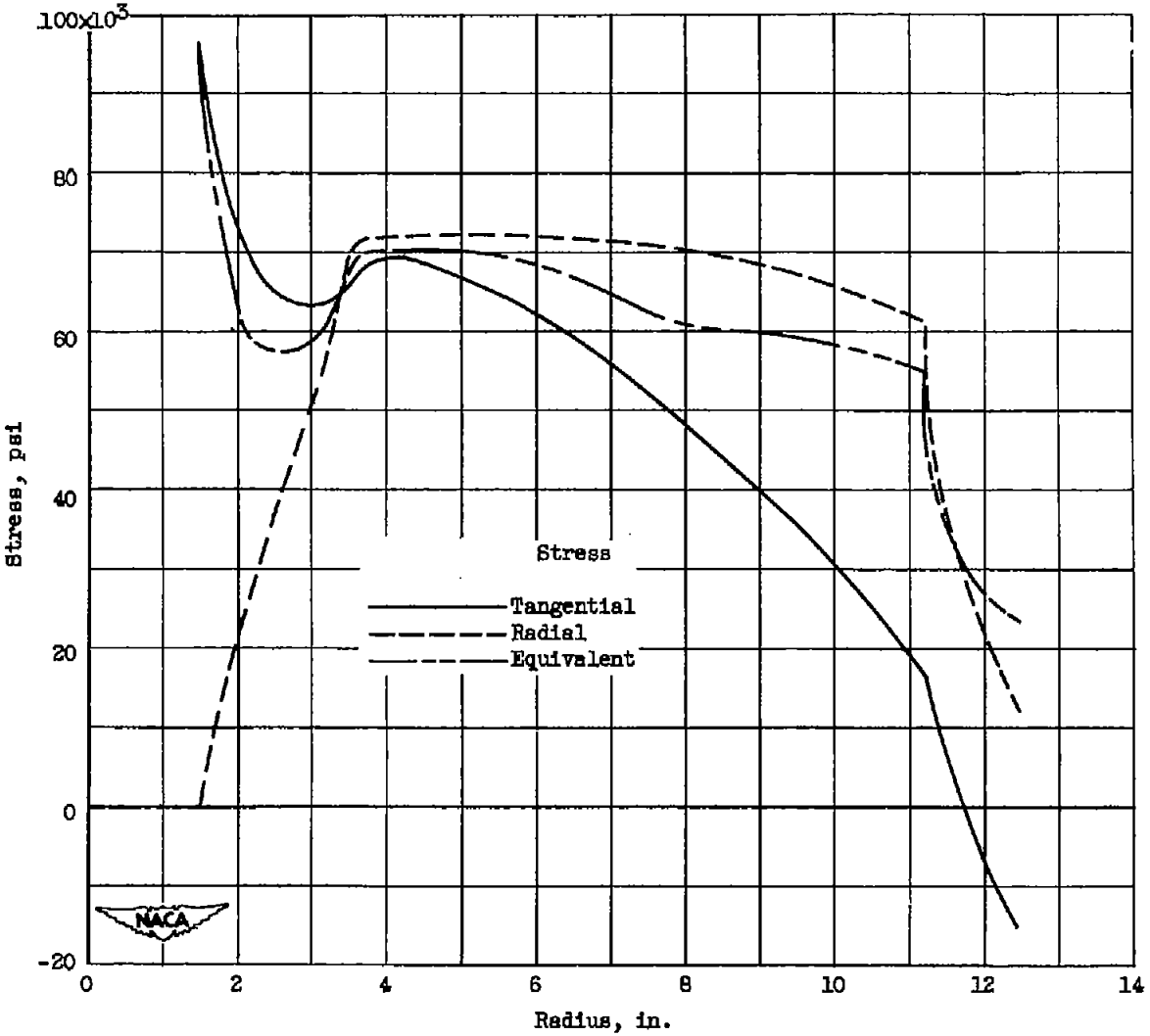

Figure 16. - Stresses in single-disk air-cooled turbine shown in figure 15.

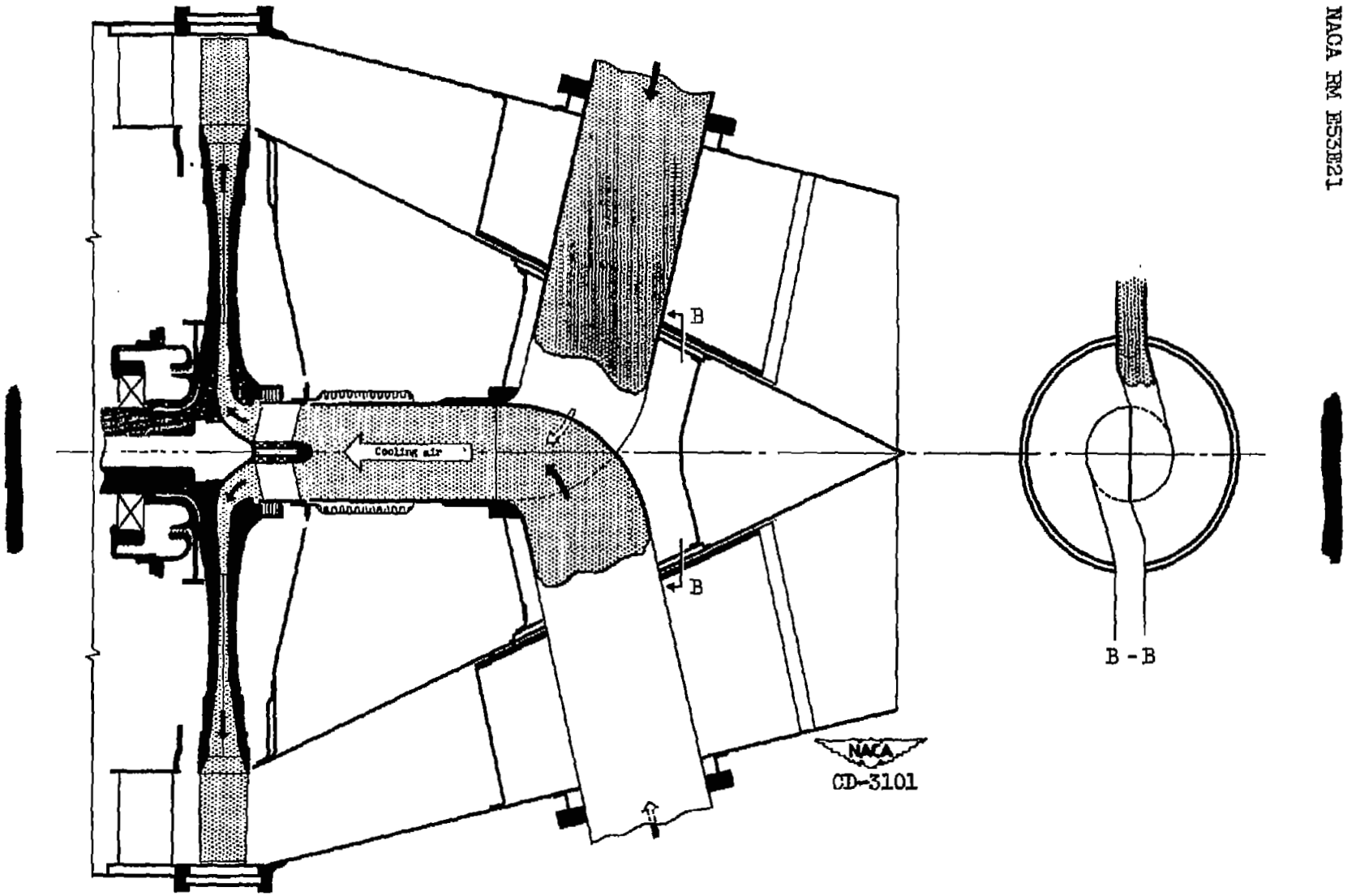

Figure 17. - Turbine assembly showing split-type air-cooled disk with cooling-air entry through tail cone.

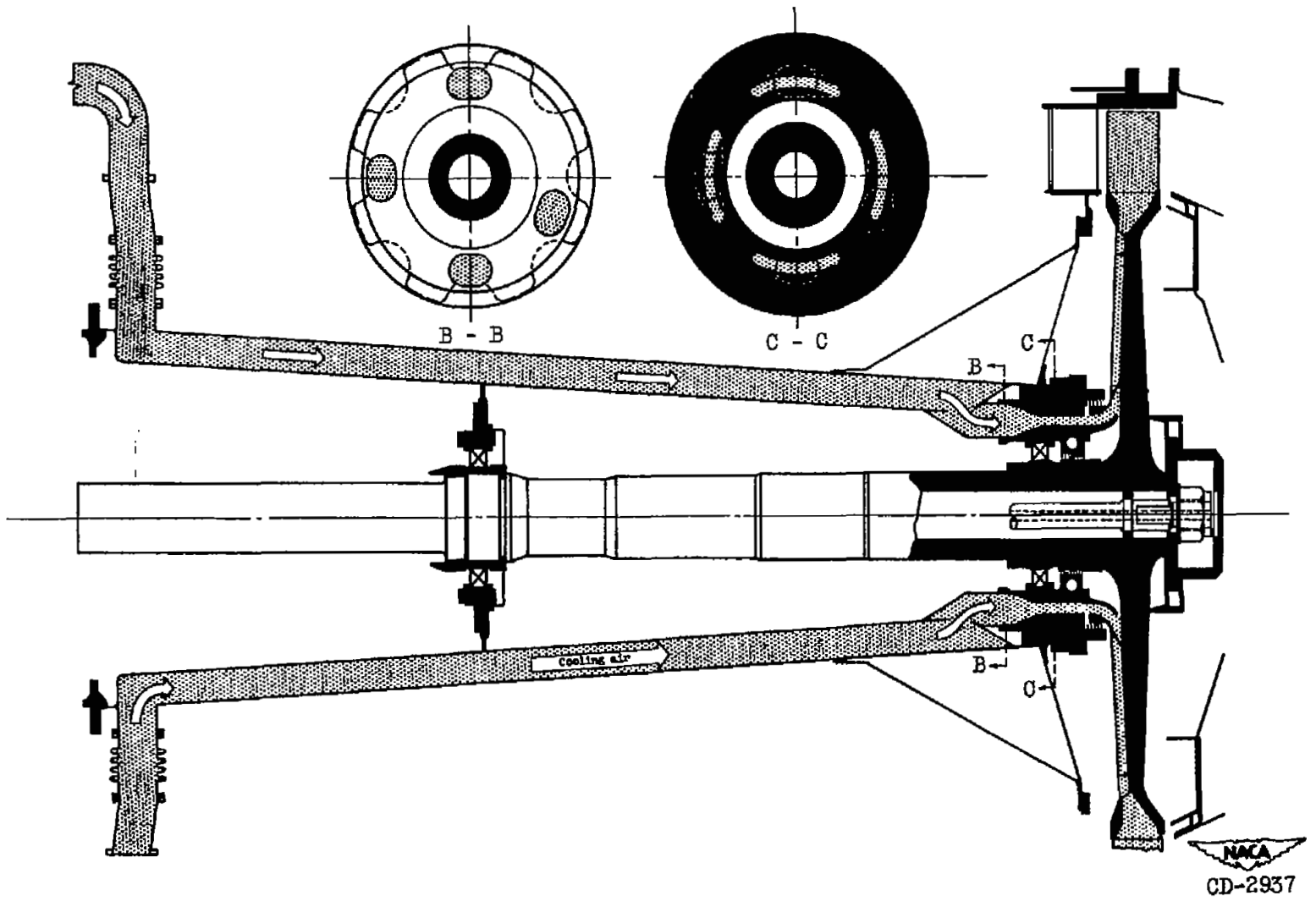

Figure 18. - Turbine assembly showing single-disk air-cooled rotor with forward-face shroud and cooling air ducted through bearing support.

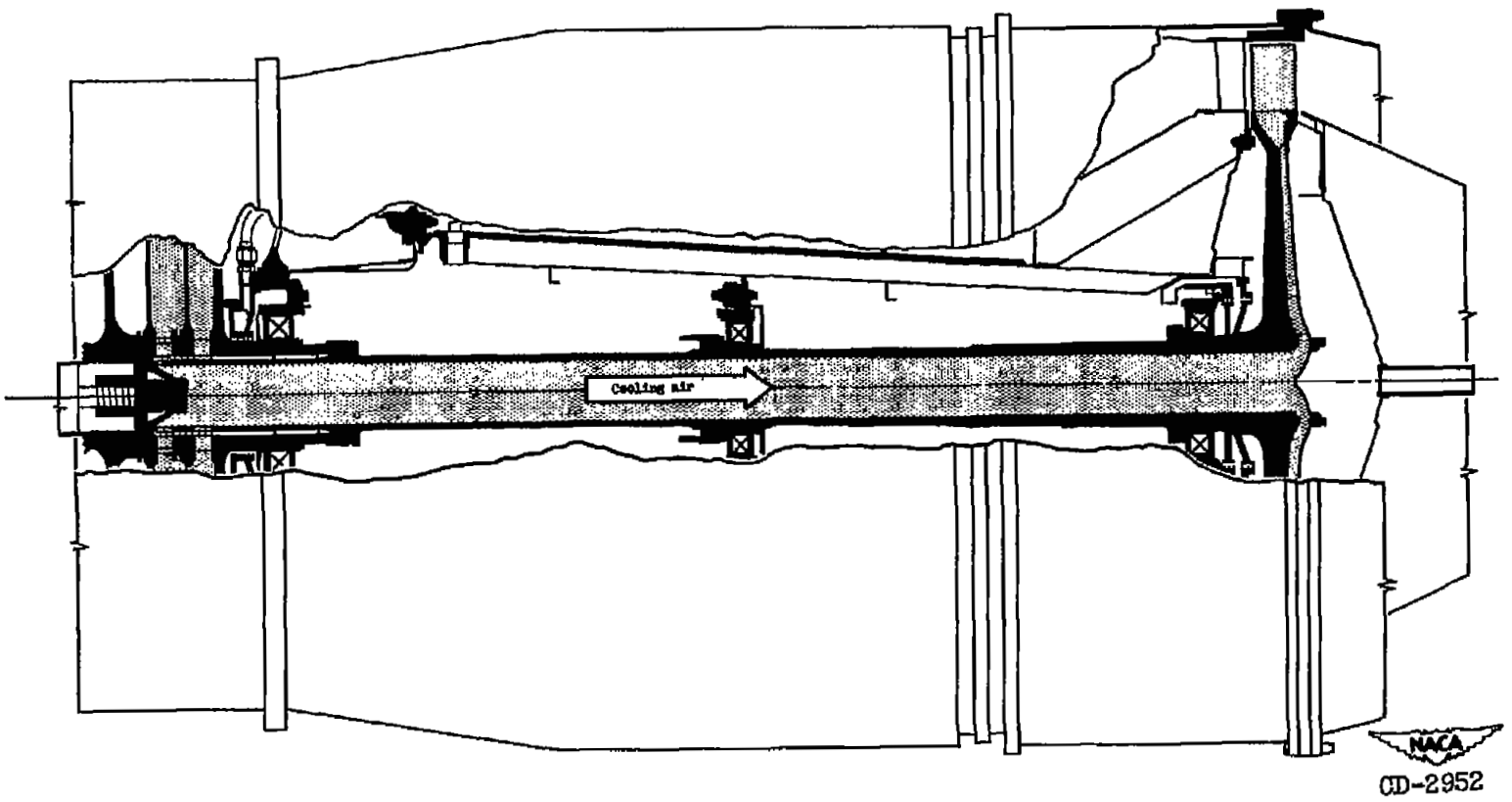

Figure 19. - Turbine assembly showing single-disk air-cooled rotor with rear-face shroud and cooling air ducted from compressor through hollow turbine shaft.

[redacted]

[redacted]

[redacted]